Spring 2017

Mass transfer studies in heavy oil recovery using solvents

Vijitha Mohan

Department: Chemical and Biochemical Engineering

MASS TRANSFER STUDIES IN HEAVY OIL RECOVERY USING SOLVENTS

by

VIJITHA MOHAN

A DISSERTATION

Presented to the Faculty of the Graduate School of the

MISSOURI UNIVERSITY OF SCIENCE AND TECHNOLOGY

In Partial Fulfillment of the Requirements for the Degree

DOCTOR OF PHILOSOPHY

in

CHEMICAL ENGINEERING

2017

Approved by

Parthasakha Neogi, Advisor

Joseph D.Smith

Joontaek Park

Fateme Rezaei

Baojun Bai

PUBLICATION DISSERTATION OPTION

This dissertation is formatted to the Missouri University of Science and Technology specifications. This report includes the following articles that has been either published or submitted for review.

Pages 14-25 include the first paper, “Flory-Huggins solution theory for heavy oils” which has been published by the *Canadian Journal of Chemical Engineering*.

Pages 26-63 include the second paper, “Concentration dependent diffusivities of model solvents in heavy oil” submitted to the *Journal of the Taiwan Institute of Chemical Engineers* for review.

Pages 64-93 include the third paper, “Revisiting Butler-Mokrys model for VAPEX process” which has been submitted to the *Society of Petroleum Engineers* for review.

ABSTRACT

Heavy oil, sometimes called bitumen, is known for its high viscosity (above 100 cp) and low API gravity (below 22^{o}). In most cases, viscosity reduction is needed for the final product. There is a considerable amount of heavy oil in Alberta, Canada and the world's largest heavy oil deposit is in Venezuela. Yet less than 1% of it can be recovered because of its high viscosity. For shallow reservoirs, it is possible to resort to open cast mining. For deeper reservoirs, steam is used at ~ 350 ºC which gets the oil viscosity reduced to 1cp, which can now be drained out. This process requires large amount of water to make steam, the used water cannot be reused due to presence of high levels of bitumen in it and is currently leading to pollution. The recovered bitumen being highly viscous needs a diluent like naphtha for transportation. Therefore another method is devised which involves using gaseous or liquid solvents directly to bring down the viscosity of bitumen. One such method, vapor extraction (VAPEX) process uses gaseous solvents like hydrocarbon solvents and CO_2 to reduce bitumen viscosity. Vaporized solvents is introduced laterally to bitumen to reduce its viscosity and the less viscous bitumen drains under gravity. Solubility of solvents in bitumen is analyzed first. As solvents solubilize, it diffuses into bitumen and the diffusivity is strongly concentration dependent. The concentration dependence of solvent diffusivity in bitumen is measured next. Knowing the solubility and diffusivity of solvents, a model is used next to simulate oil recovery. It predicts an optimum solvent for this oil recovery process.

ACKNOWLEDGMENTS

When one rules over people in righteousness, he is like the light of morning at sunrise on a cloudless morning, like the brightness after rain that brings the grass from the earth. (II Samuel 23.3)

I acknowledge my gratitude to my supervisor Professor. Parthasakha Neogi for his indefatigable mentorship. My appreciation is also extended to my research committee members, Dr.Joseph D.Smith, Dr. Joontaek Park, Dr.Fateme Rezaei and Dr.Baojun Bai.

This is dedicated to my loving grandmother who passed away this Christmas day.

TABLE OF CONTENTS

Page

LIST OF FIGURES

Page

SECTION

PAPER I

PAPER II

PAPER III

LIST OF TABLES

Page

SECTION

PAPER I

PAPER II

PAPER III

SECTION

1. INTRODUCTION

Crude oil, a fossil fuel formed from decomposition of organic matters that existed millions of years ago, accumulate within sedimentary rocks. The reservoir rocks are sandstone and carbonates. Porosity is the space in rocks that holds oil, typically ~ 0.25 and permeability of the rocks is ~ 300 mD (milliDarcy, equal to 10^{-11} cm^2) play important roles in migration and accumulation of crude oil in reservoir. Light crude oil or conventional oil which is less viscous is recovered using conventional methods. There are three stages to crude oil recovery, primary, secondary and tertiary recovery processes. First stage in the recovery process, primary recovery, depends on the natural energy in reservoir to cause oil displacement. Only 5-10% of oil can be recovered by this process. Once the pressure drops in the reservoir, recovery process stops. Second stage, secondary recovery uses external energy source like water (water-flooding) or gas injection to recover oil from the reservoir. To enhance oil displacement efficiency and volumetric sweep efficiency, there arises the need to make use of chemicals, solvents and heat. Third stage in the recovery process, tertiary oil recovery or enhanced oil recovery, uses either thermal, chemicals or miscible gases to displace remaining oil (Craig, 1971; Green & Willhite, 1998).

The depleting conventional oil reserves have led to the focus on recovering heavy oil. Generally the heavy oil fields remain untouched. Heavy oil is highly viscous and cannot be easily recovered by the above methods. After secondary recovery, when two-thirds of oil is present, enhanced oil recovery or improved oil recovery which has better reservoir management is used to recover some of this oil. It uses gases (C_1 to C_4, CO_2, N_2 and flue

gases), liquid chemicals (C_5 to C_{12}, polymers and surfactants) or thermal energy (steam or hot water). The injected fluids not only boost the natural energy in the reservoir to displace oil but also makes displacement process more stable, lowers interfacial tension, reduces oil saturation, causes oil swelling, reduces oil viscosity and modifies wettability. Heavy oil is found at various depths, in shallowest reservoir below 150 feet depth and at a reservoir temperature below 20 ^oC, in shallow reservoir below 1000 feet at a reservoir temperature of 40-60 ^oC, in intermediate depth reservoir between 1000 and 3000 feet at a reservoir temperature of 55-60 ^oC and even in deep reservoirs at 3000 feet depth and greater (Lake, 1989; Green & Willhite, 1998; Speight, 2009).

Crude oil is characterized using viscosity and American Petroleum Institute Gravity (API gravity) which is an inverse measure of density. The API gravity is expressed as follows

$$^o API = \frac{141.5}{sp.gravity} - 131.5 \quad (1)$$

The classification of crude oil based on API gravity, specific gravity and viscosity is given in Table 1.1. Water viscosity is 1 cP, Sp.Gravity is 1(^{o}API is 10) at 20 ^oC. Crude oil with API gravity greater than water will float on water and lesser than water will sink in water. Except for the variation in viscosity, almost all other properties remains the same for heavy oil and bitumen, hence the term bitumen will be used for heavy oil (Banerjee, 2012).

The average molecular weight of bitumen is difficult to determine. It varies with the solvents used and characterization methods used. Average molecular weights can be measured using gel permeation chromatography and size-exclusion chromatography. The average molecular weight of whole bitumen can be above 500 (Banerjee, 2012).

Table 1.1. Classification of crude oil using API gravity and viscosity.

Crude Oil	^{o}API	Sp.Gravity	Viscosity (cP)
Light	> 31.1	< 0.87	1 – 10
Medium	31.1 – 22.3	0.87 – 0.92	10 – 100
Heavy	< 22.3	> 0.92	100-10000
Extra heavy (Bitumen)	<10	> 1	< 10000

Surface mining was the first method used to recover bitumen. Prior to 1990s open-pit mining was done using hydraulic shovel and bucket wheels. The recovered product is transported to bitumen extraction plant through conveyor belt. It is crushed and transformed into a slurry in a hot water rotating slurry tank. Alkaline material is added to this slurry. Air is injected to achieve froth flotation and separate bitumen from sand. Separated bitumen is dehydrated and diluent is added and sent to upgrader (Banerjee, 2012).

Bitumen cannot be processed in refinery directly, hence it is transmuted to a synthetic crude through upgrading process. Upgrading involves primary and secondary

upgrading process. In the first upgrading process, bitumen is converted to low molecular weight products which is further processed in the second upgrading process to yield synthetic crude. In primary upgrading, either carbon rejection through coking or hydrogen addition through hydrocracking is done to yield a sour crude with more than 0.5% sulfur compounds. In secondary upgrading, the sour crude after primary upgrading is subjected to hydro processing to yield sweet crude with less than 0.5% sulfur compounds. The obtained synthetic crude will have 25% naphtha, 40% of distillate and 35% of VGO and no resid. Naphtha converted to high octane gasoline in naphtha reformer. Distillate sent to hydrotreater to upgrade it to diesel, kerosene and jet fuel specifications. The gas oil fraction goes to fluidized catalytic cracking (FCC) to be converted to diesel and gasoline products (Banerjee, 2012; Papavinasam, 2014; Gray, 2015).

1.1. HEAVY OIL RESERVES

Largest heavy oil reserves are found in Canada and Venezuela. In USA, heavy oil reserves are found in many states. In terms of original oil in place, large reserve is found in California (75851 million barrels). It is also found in Texas (2977 million barrels), Wyoming (1637 million barrels), Arkansas (1381 million barrels), Mississippi (1188 million barrels), Alabama (162 million barrels), Louisiana (128 million barrels) and less than 100 million barrels in Colorado, Illinois, Kansas, Michigan, Missouri, Montana, Nebraska and Utah (Nehring, 1983; Hein, 2006; Banerjee, 2012).

1.2. BITUMEN PROPERTIES

Bitumen comprises of carbon, hydrogen, oxygen, sulfur, nitrogen, metals like nickel and vanadium and asphaltene which has a high molecular weight. Properties will

vary with reservoir location. In general it may contain 15-20 vol% of distillate or atmospheric gas oil (AGO), 35-40 vol% of vacuum gas oil, 45 – 50 vol % of resid which comprises of 15-20 vol% of asphaltenes (Banerjee, 2012).

Resid or resins or residue or vacuum bottoms is a fraction that remains after vacuum distillation which is unprocessed. Asphaltenes is aromatic and defined based on their solubility nature, it is insoluble in normal-paraffin solvent (pentane and heptane) and soluble in benzene and toluene. Exact structure and molecular weight of asphaltene are unknown. Asphaltenes exact molecular weight can vary between 500 and 15000 and average molecular weight can be above 2000. Proposed structure of asphaltenes is shown in Figure 1.1. It is made up of polycondensed aromatic rings and cyclic naphthenes with sulfur, nitrogen and oxygen bonded with vanadium and nickel. Asphaltenes being heavy is believed to have made bitumen highly viscous and hindered bitumen recovery and upgrading process by contributing to fouling. Resin, like asphaltenes, is defined in terms of its solubility, resins are soluble in liquids which precipitates asphaltenes. Liquid propane and butane can precipitate resins. Resin does not have a standard structure, it is known to have a variety of hydrocarbon types and functional groups. Resins and asphaltenes may have a near similar structures with variations in aromatic carbons. Resin and asphaltene interaction appear to be strong compared to individual interactions. It is predicted that resins layers could have been adsorbed on asphaltenes (Speight, 2004; Banerjee, 2012; Aguiar, 2015).

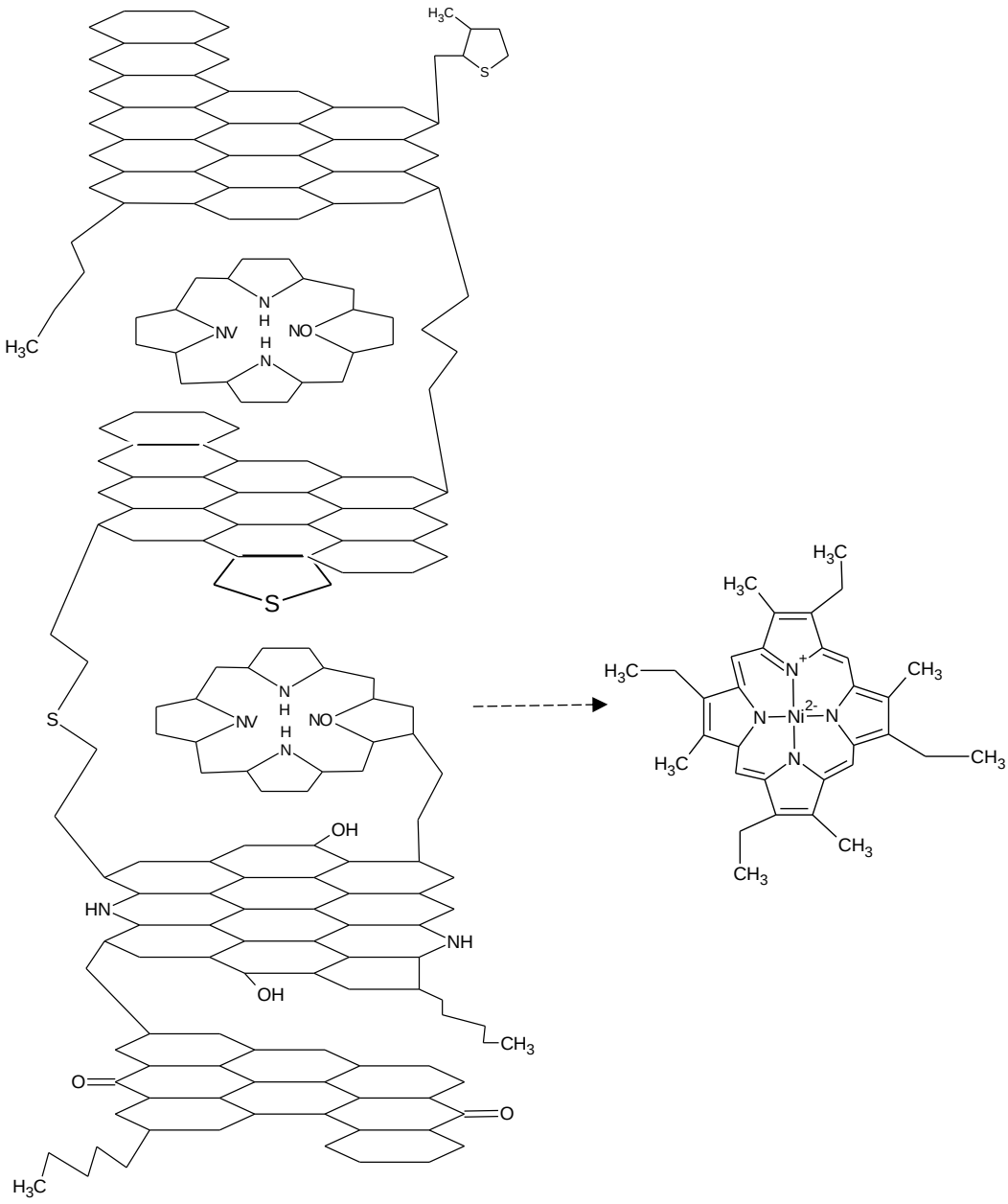

Figure 1.1. Proposed structure of asphaltene (http://what-when-how.com/petroleum-refining/upgrading-of-heavy-feeds-part-1-petroleum-refining/).

The elemental composition of bitumen and further classifications SARA and PONA using solvent extraction method are as follows.

1.2.1. Elemental Composition. Bitumen consists of high level of hydrocarbons and sulfur, nitrogen, oxygen and metals. It consists of more than 80 wt% carbon and 10 wt% hydrogen.. The hydrogen to carbon atomic ratio shows the quality of crude, higher the ratio, better the quality. Bitumen hydrogen to carbon ratio is 1.4-1.5. High sulfur and nitrogen content may make processing expensive and detrimental. Expected elemental and metal composition of Alberta bitumen is given in Table 1.2 (Subramanian et.al, 1996; Banerjee, 2012).

Table 1.2. Expected elemental and metal composition of Alberta bitumen.

Element	Range (wt %)	Element	Range (ppm)
Carbon	82.1- 83.0	Nitrogen	3000 – 5000
Hydrogen	10.1- 10.2	Vanadium	180 – 250
Sulfur	4.5- 6.0	Nickel	60-90
Oxygen	< 1.0		

1.2.2. SARA Classification. Column chromatography was employed to classify bitumen in terms of saturates, aromatics, resins and asphaltenes using various adsorbing materials and solvents. Saturated involves saturated carbon atoms. Aromatics involves unsaturated benzene rings. The weight percentage will vary with location. Bitumen is first separated into solid asphaltenes and maltenes dissolved in n-paraffin solvent. Maltenes

further separated using pentane as resins and oils. Oil further separated as colored aromatics and colorless saturates. Alberta bitumen is known to contain more resins than saturates and aromatics. Gel permeation chromatography can be used to obtain average molecular weights and it follows the order, Asphaltenes > Resins > Aromatics > Saturates. Its general weight percentage and weight percentage in Alberta bitumen is given in Table 1.3 (Speight, 2009; Banerjee, 2012).

Table 1.3. SARA classification.

Fractions	Weight % (General)	Weight % (Alberta)
Saturates	15 – 20	1 - 2
Aromatics	30 – 35	5 - 8
Resins	25 – 30	50 – 55
Asphaltenes	15 – 20	30 - 35

1.2.3. PONA Classification. PONA stands for Paraffins, Olefins, Naphthenes and Aromatics. Paraffins consists of single bond carbon atoms saturated with hydrogen. Olefins consists of some carbon double bond atoms. Naphthenes are cycloparaffins with carbon atoms saturated with hydrogen. High performance liquid chromatography was used to characterize the distillate fraction of bitumen excluding the resid portion. Aromatics is higher even in the non-resid portion and high aromatic nature will degrade bitumen quality.

A typical PONA classification is give in Table 1.4 and again the classification is specific to location (Speight, 2009; Banerjee, 2012).

Table 1.4. PONA classification.

Fractions	Weight %
Paraffins	< 10
Olefins	< 10
Naphthenes	20 – 30
Aromatics	60 – 70

1.3. OIL RECOVERY METHODS FOR HEAVY OIL

There are three main techniques, thermal recovery, gas injection and chemical injection. Thermal methods uses heat in the form of steam injection namely like steam assisted gravity drainage (SAGD) and cyclic steam stimulation (CSS) process. SAGD and CSS are similar process, in SAGD process steam is introduce to form a steam chamber to interact with heavy oil whereas CSS includes a huff and puff mode. Toe-to-Heel Air Injection (THAI) is another thermal process which involves in situ combustion. Gas injection involves injecting natural gas, carbon dioxide and other vaporized solvents. Vapor Assisted Petroleum Extraction (VAPEX) is one such process where vaporized solvents or gas introduced to reduce bitumen viscosity. Chemical injection involves injecting long chained polymers or surfactants to decrease surface tension and enhance

bitumen movement (Speight, 2009; Banerjee, 2012; Papavinasam, 2014; Alagorni et.al, 2015).

1.3.1. SAGD. Steam Assisted Gravity Drainage (SAGD) process is the most popular thermal method used for recovering bitumen. SAGD is found to be more effective in Alberta than in USA and Venezuela. Butler (1991) developed the technology in the 1970s however it received recognition only in 1990s. This process involves two L-shaped wells, upper injection well and lower production well. It involves passing steam into the reservoir to heat up bitumen and reduce its viscosity and collect the drained bitumen by gravity. The horizontal wells placed one above the other 5 m apart, the top well carries the steam at temperature above 300 ^{o}C and pressure above 3000 kPa creating a steam chamber. Continuous injection of steam makes the steam chamber to expand. The steam heats up bitumen and reduces its viscosity to 1cP which drains under gravity to the bottom well. This process is suitable for bitumen with low mobility as steam chamber is desired over steam channels for efficient reduction of oil viscosity. The bottom well carries both bitumen and condensed steam back to the surface. It is important that the production well be well situated at the bottom of steam chamber in a correct position to collect the mobilized bitumen. During the beginning of the process, steam is circulated through both injection and production wells to heat the bitumen around the wells through thermal conduction. Once fluid communication is reached between the wells, steam injection is only through the injection well and production well is used for oil collection only. Major drawback in this process is it is highly energy intensive and it requires large volumes of water to convert it to steam and natural gas is used as a fuel. It also involves CO_2 emission. Pressure difference of at least 200 psi is required to lift the product more than 300m to the

surface. The recovered water cannot be reused as it may contain traces of bitumen in it. The time required to heat the steam chamber is long about three to four months. Schematics of SAGD process shown in Figure 1.2 (Butler, 1991; Thomas, 2008; Speight, 2009; Banerjee, 2012; Papavinasam, 2014).

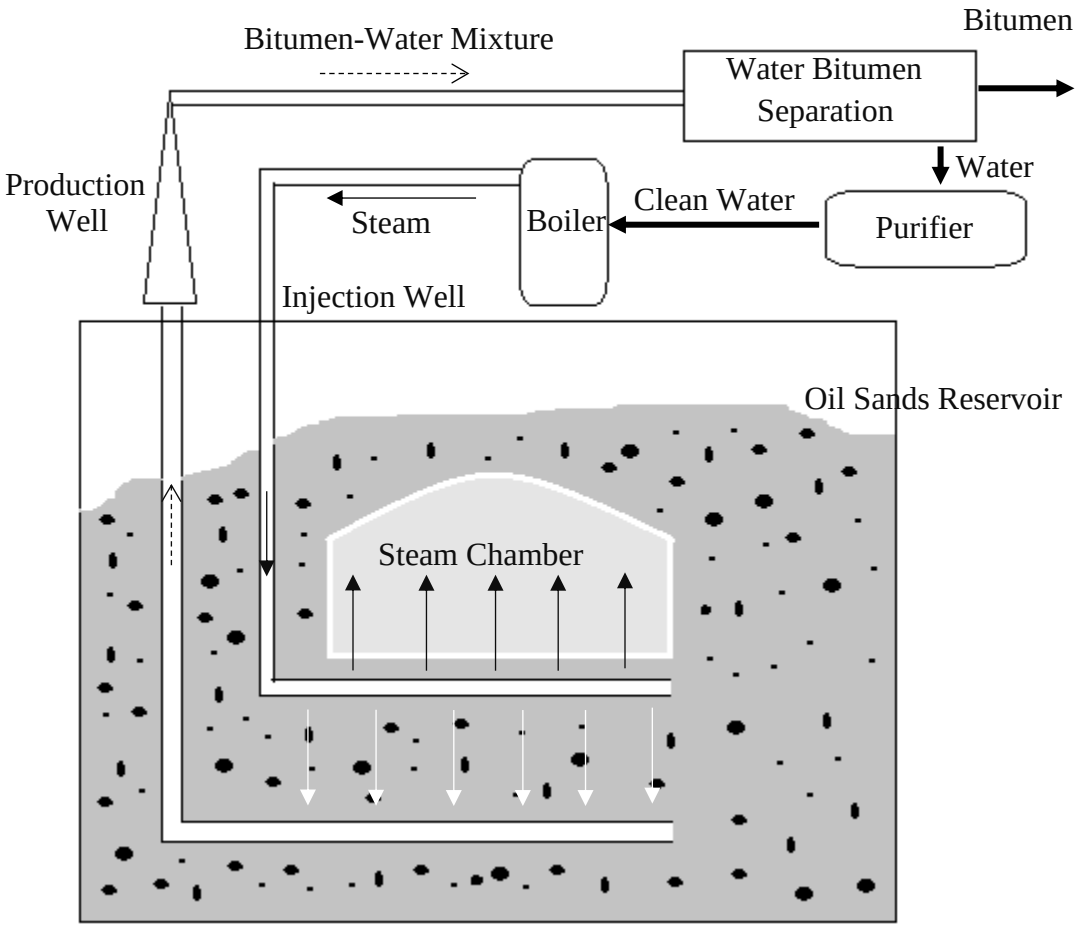

Figure 1.2. Schematic diagram of SAGD process .

1.3.2. CSS. Cyclic Steam Stimulation (CSS) is a three phase thermal process in a single well, also known as huff and puff method. In the first phase or huff, a high pressure steam is injected in to the reservoir for 4 to 6 weeks. In the second phase, steam injection is stopped and the injected steam is allowed to form a steam chamber for 2 to 8 weeks. Bitumen gets heated up and becomes less viscous. In the third phase or puff, bitumen is pumped out. A process that may take several months. Recovery process is slow. Schematics shown in Figure 1.3 (Speight, 2009; Banerjee, 2012; Papavinasam, 2014).

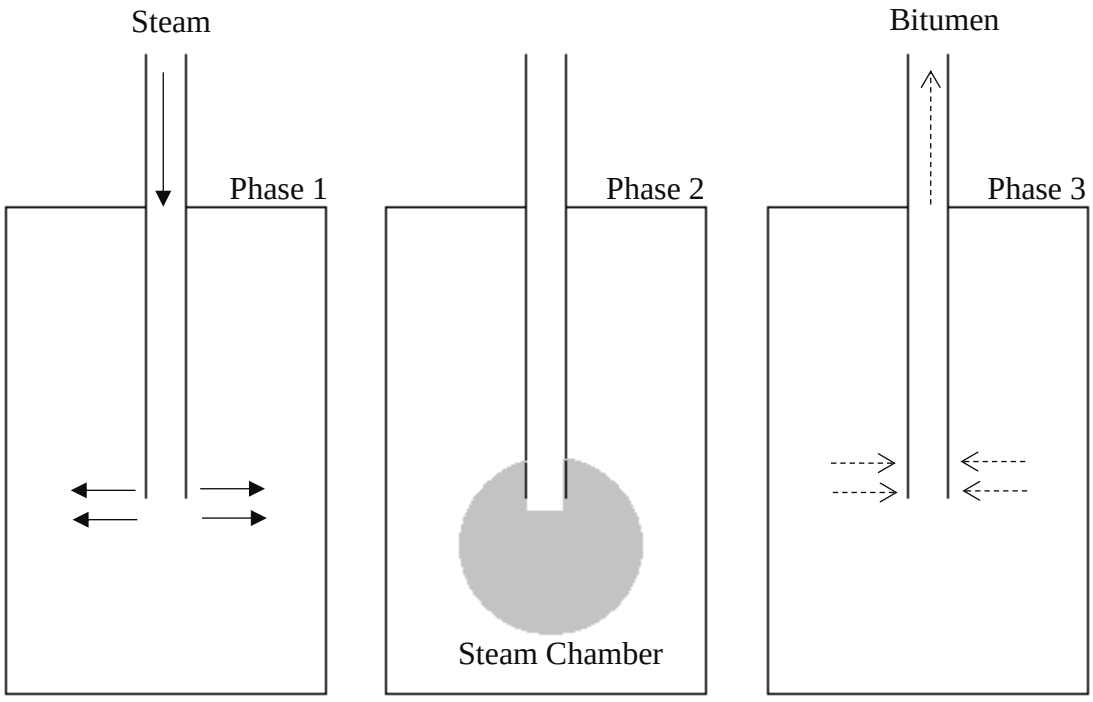

Figure 1.3. Schematic diagram of CSS process.

1.3.3. VAPEX. Vapor Assisted Petroleum Extraction (VAPEX) is a non-thermal process. It is analogous to SAGD process using two horizontal wells where vaporized solvent is used instead of steam. Injected solvent creates a solvent chamber, interacts with bitumen reducing its viscosity. The less viscous bitumen drains by gravity into production well. Being a non-thermal process, fuel is not required for burning and hence reduced greenhouse gas emissions. The used solvents can be recovered and reused. One of the main advantages in this process is no water usage and hence the process is not expensive and does not cause any pollution. This process can also be used for CO_2 sequestration. (Speight, 2009; Banerjee, 2012; Papavinasam, 2014).

1.4. THESIS PLAN

In a process like VAPEX, taking oil to be a zero component solubility of solvents in it can be easily analyzed just by using volume fraction of solvents. Diffusion of solvents in bitumen displays strong concentration dependence than ordinary diffusion. The solubility studies is discussed in the first paper "Flory-Huggins solution theory for heavy oils." The diffusion studies is discussed in the second paper "Concentration dependent diffusivities of model solvents in heavy oil." Understanding the solubility and diffusion characteristic of solvents in bitumen, choosing an optimum solvent for this solvent induced oil recovery is discussed in the third paper "Revisiting Butler-Mokrys model for VAPEX process." Butler and Mokrys (1989) scheme is revisited and modified by creating a concentration equation and then obtaining a concentration profile of the solvent in oil. Using the concentration profile, an optimum solvent can be predicted.

PAPER

I. FLORY-HUGGINS SOLUTION THEORY FOR HEAVY OILS

Vijitha Mohan,[1] Parthasakha Neogi[1] and Baojun Bai[2]

[1] Chemical and Biochemical Engineering,

[2] Geosciences and Geological and Petroleum Engineering,

Missouri University of Science and Technology, Rolla, MO 65409-1230, USA

ABSTRACT

The addition of a solvent to heavy crude oil causes reduction in its viscosity and facilitates extraction. Existing data on swelling of oil in presence of solvent in vapor form have been analyzed using Flory-Huggins theory. The model uses volume fractions and hence problems related to what an appropriate average molecular weight of oil to use in the calculations are avoided. The data expressed in terms of swelling as a function of solvent partial pressure fits well with the model when the solvent vapor can condense and is miscible with oil or immiscible with oil or even when condensation is not possible. We are also able to predict when phase separation can occur (which we take to be asphaltene precipitation) in the solution although the above experiments have not looked at this aspect.

NOMENCLATURE

Symbol	Description
b	constant
f_w	swelling factor
p	pressure (MPa)
p_v	vapor pressure (MPa)
R	gas constant (kg m^2 mol^{-1} K^{-1} s^{-2})
T	temperature (K)
μ^o	standard state chemical potentials
μ_L^o	standard state chemical potential in liquid form
μ_V^o	standard state chemical potential in vapor form
ϕ	volume fraction of the solvent in the crude
ϕ_o	volume fraction at p_V
χ_1	flory-Huggins coefficient

1. PROLOGUE

Solubility of solvents in heavy oil is analyzed using gaseous solvents. Hydrocarbons C_1 to C_7, toluene, benzene and carbon dioxide can be used as solvents. As solvents solubilize in oil, it causes viscosity reduction, swelling of oil and asphaltene solubility or precipitation. Solvents like n-alkanes and CO_2 cause asphaltene precipitation but not toluene and benzene. In a reservoir, swelling of oil leads to oil being pushed out of the reservoir pores and hence measuring swelling is a way to quantify the amount of oil recovered. Crude oil is taken to be a single pseudo-component. In this study, Flory-Huggins theory is used to create a model that can predict swelling behavior of oil and asphaltene precipitation in the presence of gaseous solvents. Flory-Huggins theory model uses volume fraction of solvents and does not require using molecular weight of the heavy oil. This model is used for gaseous solvents, ethane, propane, carbon dioxide and methane. These solvents solubilized in heavy oil at various pressures and at room temperature. Gaseous solvents once solubilized in heavy oil condenses into a liquid form (Prausnitz et al, 1999). In general, liquid ethane and propane is miscible in heavy oil whereas liquid CO_2 is immiscible in heavy oil. Critical temperature of methane is below room temperature. The model's predicted swelling characteristics of oil in the presence of these four solvents fitted well with experimental data and the model also predicts when asphaltene precipitation would occur (Simon and Graue, 1965; Mulliken and Sandler, 1980; Butler and Mokrys, 1991; Buenrostro-Gonzalez et al, 2004; Painter et al, 2015).

2. INTRODUCTION

In the solvent-vapor extraction (VAPEX) process for heavy oils, a vapor is dissolved in the oil such that resultant oil has a lower viscosity and drains under gravity to the production well. It is important to understand the solubility of a gas or vapor in oil. A schematic diagram of the process is shown in Figure 2.1 using horizontal wells (Butler and Mokrys, 1991). In either case the dissolved solvent is considered to be in a condensed state.

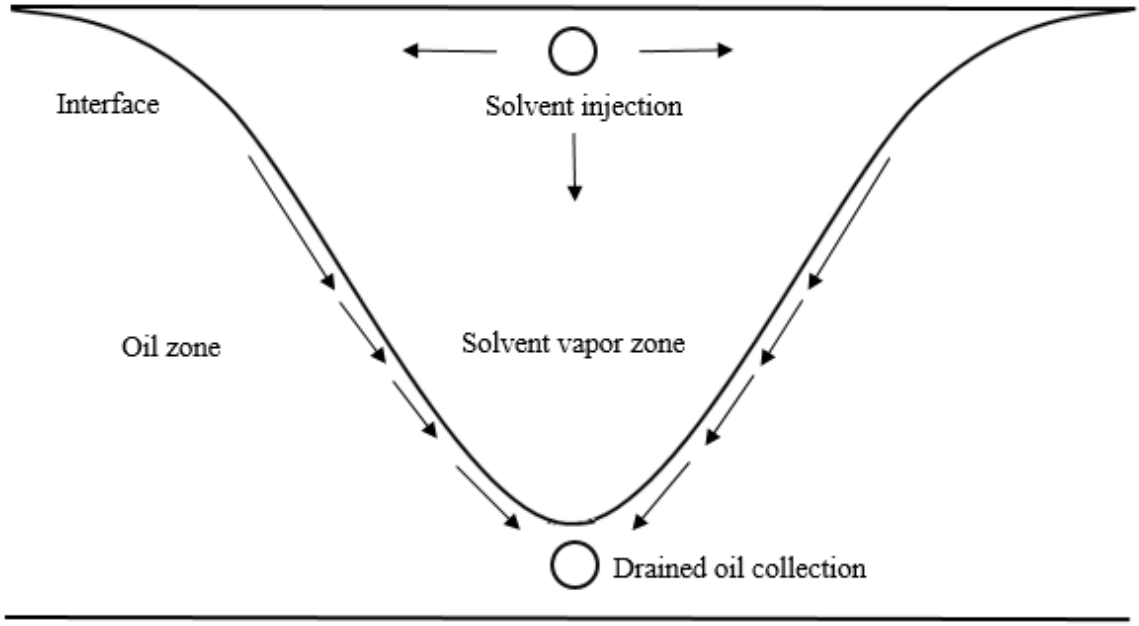

Figure 2.1. Schematic diagram of solvent – vapor extraction (VAPEX) process for heavy oils (Butler and Mokrys, 1991).

The major problem with most thermodynamic relations is that the molecular weight of oil is needed. Banerjee describes how various methods give us a very wide range for values of average molecular weights (Banerjee, 2012). The method of breaking oil down into components to obtain a mole averaged value is laborious and it is not clear whether

averaged values with different weights may not be needed to describe other properties. On the other hand some have stressed that in the use of Flory-Huggins equation which uses volume fractions, the entire issue of molecular weights is circumvented (Mullins et al, 2007).

The chemical potential of the solvent in the crude oil is expressed using Flory-Huggins theory (Flory, 1953) and equated to the chemical potential of the vapor to get the following

$$\mu_L^o + RT\{\ln\phi + (1-\frac{1}{x})(1-\phi) + \chi_1(1-\phi)^2\} = \mu_V^o + RT\ln p \quad (1)$$

where μ^o are the two standard state chemical potentials, ϕ is the volume fraction of the solvent in the crude, x is the number of sites occupied by a molecule of crude relative to one molecule of the solvent, χ_1 is the Flory-Huggins coefficient, and p is the vapor pressure of the of solvent. The Flory-Huggins theory is a lattice theory for polymer solutions, where a solvent molecule occupies a single lattice site and the polymer repeat unit occupies a single site. It was found that the connectivity between adjacent sites does not play a role, nor do repeat units or size of the solvent molecules define the size of a site. As a result, the left hand side of Equation. 1 is relatively independent of molecular weights or molecular weight distribution or the architecture of the molecules, as long as the ratio between the polymer molecular weight and solvent molecular weight is large (x). Most remarks on polymers in the above can be extended directly to heavy oils. The key achievement in Flory's theory was to replace activity which is the mole fraction (nearly) with volume fraction (nearly). In systems with disparate molecular weights, mole fractions have

unseeming magnitudes whereas volume fractions are reasonable. Since the vapor is condensable, at $\phi = 1, p = p_v$ and Equation. 1 becomes the following

$$\mu_L^o = \mu_v^o + RT \ln p_v \tag{2}$$

Subtracting Equation. 2 from Equation. 1 and simplifying, we get the following:

$$\ln \phi + (1 - \frac{1}{x})(1 - \phi) + \chi_1 (1 - \phi)^2 = \ln p / p_V \tag{3}$$

Now to 1cm^3 of oil, if we add u cm^3 of solvent (liquid), we have $\phi = \frac{u}{1+u}$ and the swelling is defined as $f_w = \frac{1+u}{1}$ assuming that volumes are additive. Combining the two, we have the following:

$$f_w = 1 + \frac{\phi}{1-\phi} = \frac{1}{1-\phi} \tag{4}$$

It is possible to combine Equations. 3 and 4 to write f_w as a function of p / p_V. Equation. 4 predicts a curvature in f_w versus p / p_v and the data of Yang and Gu, 2006 do show curvatures in the ethane and propane data in Lloydminister heavy oil but their plotted data on carbon dioxide and methane show no curvatures. The data of Chung et al, 1988 show that even when carbon dioxide condenses, the liquid CO_2 is not miscible with oil (Bartlett heavy oil). For methane, the critical temperature is below the working temperature and as a result no condensation will take place and a saturated vapor pressure p_v of 31.38 MPa reported by them is taken here to be only a reference pressure. In such cases the limit used above that $\phi \to 1$ as $p \to p_v$ cannot be applied, instead $\phi \to \phi_o$ in that limit. For this case Equation. 3 becomes the following:

$$\ln\phi + (1-\frac{1}{x})(1-\phi) + \chi_1(1-\phi)^2 = \ln(b.p\ /\ p_V) \quad (5)$$

where the constant $b = p_v e^{(\mu_V^o - \mu_L^o)/RT}$ is very similar to Henry's law constant. If we take the logarithm after substituting the expression for b into Equation. 5, we get back Equation. 6. Further, the above limit gives us the following:

$$\ln\phi_o + (1-\frac{1}{x})(1-\phi_o) + \chi_1(1-\phi_o)^2 = \ln b \quad (6)$$

Equation. 5 is used to calculate parameters x, χ_1, and b, and Equation. 6 to calculate ϕ_o .

3. RESULTS AND DISCUSSION

The fitted curves and data from Yang and Gu, 2006 are shown below first for ethane and propane (miscible) in Figure 3.1 and for methane and CO_2 in Figure 3.2. Shown in Table 3.1 are all the physical properties data including some that are obtained through curve fitting. Note that in all cases x is practically infinite. Flory has provided a number of experimental measurements on χ_1 for polymer solutions and except for special circumstances, the values are bunched around 0.3 (Flory, 1953). Note that in Equation. 3 if we take x to be infinite beforehand, we can get χ_1 as a function of ϕ, one pair for every data point.

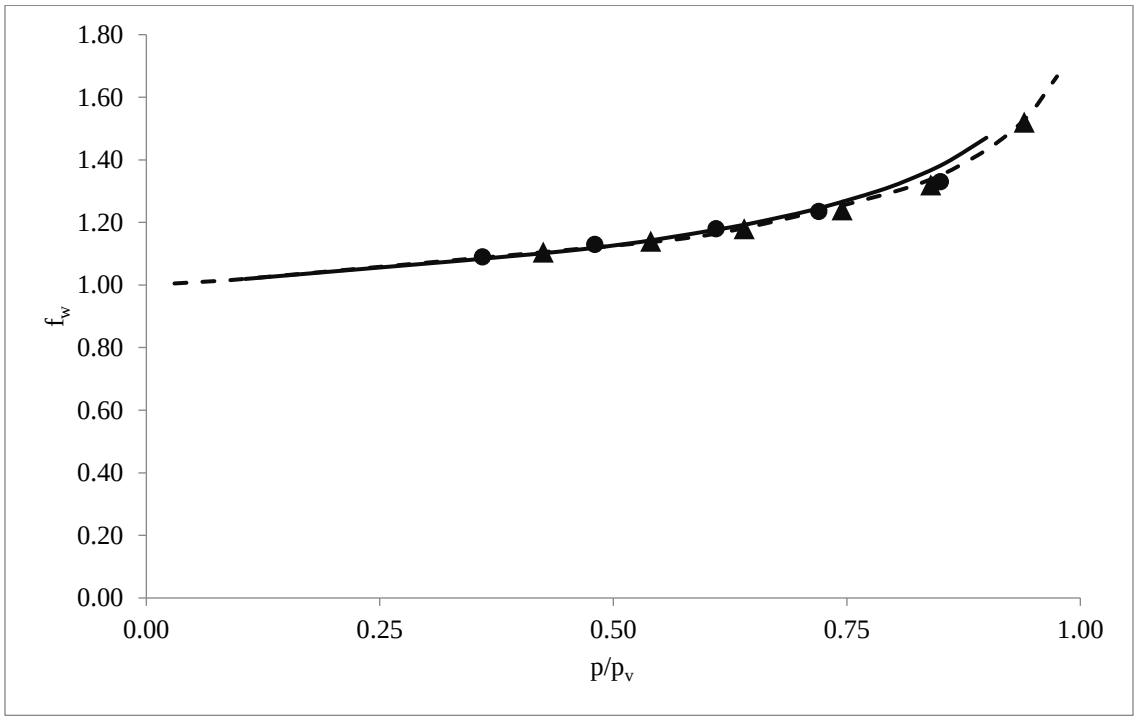

Figure 3.1. Swelling data and the fit to Equation. 3 are shown. The parameters are reported in Table 3.1. It is assumed that the condensed solvent at that temperature 297.1K is miscible with oil. Circle and bold line for ethane and triangle and dashed line for propane.

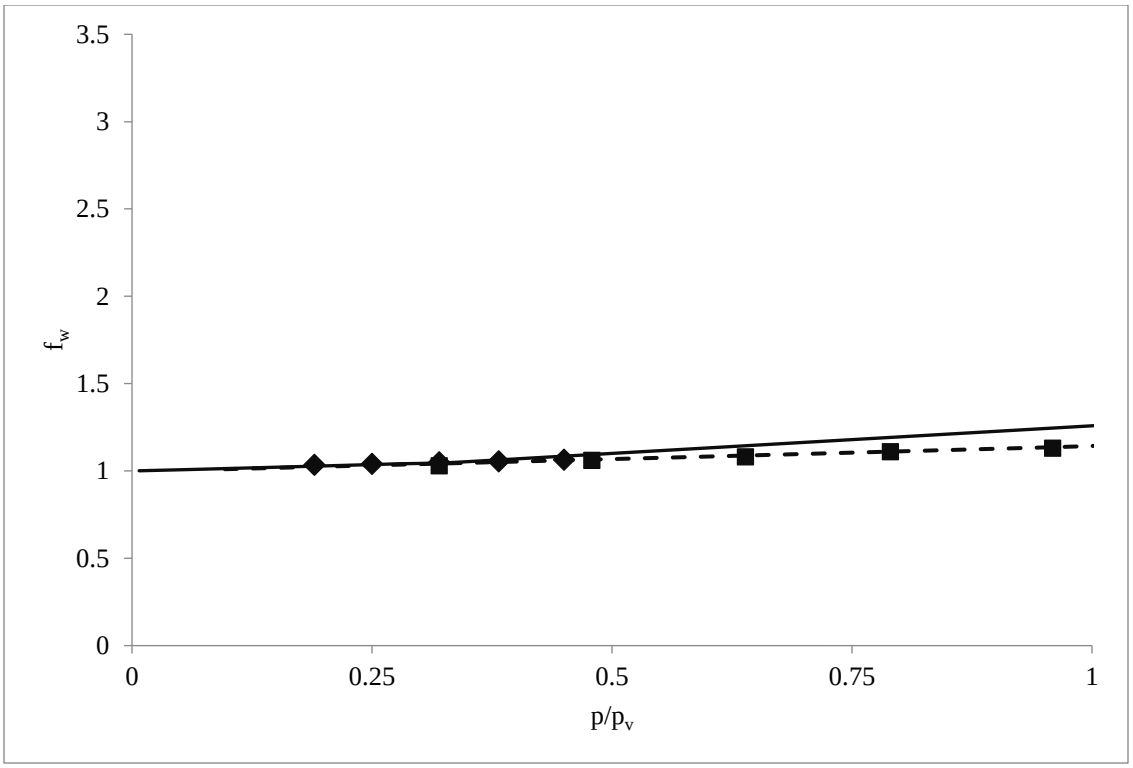

Figure 3.2. Swelling data and the fit to Equation. 5 are shown. The parameters are reported in Table 3.1. It is assumed that condensed CO_2 (square and dashed line) at 297.1K is immiscible with oil, and for CH_4, a pressure of 31.38 MPa is a standard pressure (diamond and bold line). Methane cannot condense at this temperature.

This has not been undertaken because we only see in the data beginnings of concentrated behavior. Hence the use of an average value is reasonable. For fitting data to Equation. 5, we have another constant and have to be satisfied with an average where the concentrations are all low and below ϕ_o. The values of Flory-Huggins coefficients in Table 3.1 for ethane and propane are more than 0.5, which says that the solution is unstable. We take it mean that asphaltene will precipitate. The highest value of solvent volume fraction in case of CO_2 is 0.126 and in the analysis of Tran et al, 2012 of data by Chung et al, 1988

it is seen to go up to almost 0.35, but the pressures used by Chung et al, 1988 are also very high (up to 34.47 Mpa). For CO_2 and methane, b is less than 1.0, which effectively reduces the gas phase activity.

Table 3.1. Notable physical properties of the four gases and vapors including solution properties determined here at 297.1K.

	CO_2	CH_4	C_2H_6	C_3H_8
T_c K	304.2	190.7	305.4	369.9
p_v MPa	6.28	31.38	4.12	0.93
v_L cm^3/g	1.06[b]	3.25[c]	1.81[d]	1.43[d]
x[a]	5000.0	99999.0	100002.3	100003.9
χ[a]	0.384	0.081	0.764	0.808
b[a]	0.405	0.400	1	1
ϕ_o	0.126	0.164	1	1

a Fitted, b Tran et al, 2012, c Prausnitz et al, 1999, d Prausnitz et al, 1999 at infinite dilution

4. CONCLUSIONS

Flory-Huggins equation fits well the data on the swelling of heavy crude oil molecule by carbon dioxide, methane, ethane and propane. Here ethane, propane and carbon dioxide are below their critical temperatures and in the liquid form ethane and propane are miscible with oil, but carbon dioxide is immiscible with oil and methane is above its critical temperature. Thus, the solution theory is quite versatile, gives appropriate values of the parameters and even suggests when phase separation in the solution (which we take to be asphaltene precipitation) can happen.

REFERENCES

Banerjee, D.K. (2012) Oil Sands, Heavy Oil and Bitumen, From Recovery to Refinery, Penn Well Corp, Tulsa.

Butler, R.M., and Mokrys, I.J. (1991) A new process (VAPEX) for recovering heavy oils using hot water and hydrocarbon vapor, The Journal of Canadian Petroleum Technology, 30, 1, 97-106.

Flory, P.J. (1953) Principles of Polymer Chemistry, Cornell University Press, Ithaca, p. 541.

Buenrostro-Gonzalez, E., Lira-Galeana, C., Gill-Villegas, A., and Wu, J. (2004) Asphaltenes Precipitation in crude oils: theory and experiments, American Institute of Chemical Engineers Journal, 50, 10, 2552-2570.

Mullins, O.C., Shen, E.Y., Hammam, A., and Marshall A.G. (2007) Asphaltenes, Heavy Oils, and Petreomics, Springer, New York, p. 303.

Mulliken, C.A., and Sandler, S.I. (1980) The prediction of CO_2 solubility and swelling factors for enhanced oil recovery, Industrial &.Engineering Chemistry, 19, 709-711.

Painter, P., Veytsman, B., and Youtcheff, J. (2015) Guide to asphaltene solubility, Energy & Fules, 29, 2951-2961.

Simon, R., and Graue, D.J. (1965) Generalized correlations for predicting solubility, swelling and viscosity behavior of CO_2-crude oil systems, Journal of Petroleum Technology, 102-106.

Yang, C., and Gu,Y. (2006) Diffusion coefficients and oil swelling factors of carbon dioxide, methane, ethane, propane and their mixtures in heavy oil, Fluid Phase Equilibria, 243, 64-73.

Chung, F.T.H., Jones, R.A., and Nguyen, H.T. (1988) Measurements and correlations of the physical properties of CO_2/heavy-crude-oil mixtures, SPE Reservoir Engineering, 3, 822-828.

Tran, T.Q.M.D., Neogi, P., and Bai, B. (2012) Free volume estimates of thermodynamic and transport properties of heavy oil with CO_2, Chemical Engineering Science, 80, 100-108.

Prausnitz, J.M., Lichtenthaler, R.N., and De Azevedo. E.G. (1999) Molecular Thermodynamics of Fluid Phase Equilibrium, 3rd edition, Prentice-Hall Inc, New Jersey, p. 607.

II. CONCENTRATION DEPENDENT DIFFUSIVITIES OF MODEL SOLVENTS IN HEAVY OIL

Vijitha Mohan,[1] Parthasakha Neogi[1] and Baojun Bai[2]

[1] Chemical and Biochemical Engineering,

[2] Geosciences and Geological and Petroleum Engineering,

Missouri University of Science and Technology, Rolla, MO 65409-1230, USA

ABSTRACT

The rates of dissolution of heavy crude oil in liquid solvents and rates of desorption of solvents from oil have been measured. The crude oil used is a non-volatile heavy oil of 4253 mPa.s viscosity at room temperature. The solvents used are hexane, heptane and toluene. When the oil (black) is contacted with a solvent (transparent) an interface is seen which moves with time and takes a very long time to become fuzzy. This sharp interface in a miscible system is attributed to a very strongly concentration dependent diffusivity. The mathematical solution to the problem can then be used to calculate the diffusivity as $D_o e^{\alpha\phi}$ where ϕ is the volume fraction of the solvent. The dissolution experiments give very consistent results, but there are two parameters involved, D_o, the diffusivity at infinite dilution and α which determines the concentration dependence. The dissolution experiments themselves are not able to determine both parameters. Consequently, desorption experiments were performed, but could not be performed under conditions suitable for the present case because of the very viscous nature of the oil. As a result, although the desorption experiments also showed good results, they could not be used to obtain good values of the parameters. When Stokes-Einstein equation was used to

calculate D_o, excellent results were obtained for $\alpha \sim 10$. That result is used to conclude that the above form for concentration dependent diffusivity is correct and concentration dependence is very high explaining the sharp interfaces during dissolution. There are additional evidence.

NOMENCLATURE

Symbol	Description
a	radius of the solvent molecule
D	Diffusivity
D_o	Diffusivity at infinite dilution
f	free volume fraction of polymer
g	free volume fraction of penetrant
k_B	Boltzmann constant
p	slopes of location versus √time
Δx_o	amount by which the interface has moved
t	time
v_o	specific volume of solvent
α	concentration dependent term
λ	product of density of oil and specific volume of solvent
μ_o	viscosity of the uncontaminated oil
ρ_o	density of oil
σ	Lennard-Jones potential
ϕ	volume fraction of the solvent in the crude
ϕ_∞	saturation volume fraction of the solvent

1. PROLOGUE

As solvents solubilized in heavy oil, the movement of solvents in heavy oil is caused by diffusion. The diffusivity of diffusing solvents depends on the concentration of diffusing solvents, temperature and pressure. In dilute systems, diffusivity highly depend on the concentration of diffusing substance whereas in concentrated systems diffusivity is not that much dependent on the concentration of diffusing substance. This study is to prove that the diffusivity of solvents in heavy oil is strongly dependent on the concentration of solvents used. As reported in the previous study, gaseous solvents in heavy oil will condense into liquids, therefore liquid solvents are directly used for studying concentration dependence in heavy oil. Hydrocarbon solvents C_6 to C_{12}, toluene and benzene can be used as solvents. Hexane, heptane and toluene are used as solvents and a Kansas heavy crude oil is used. As solvents comes into contact with the heavy oil, heavy oil being highly viscous, an interface is observed in the absence of mixing. The movement of interface with time is monitored. A model is created to relate the movement of interface to concentration dependence of diffusivity. Asphaltene is known to precipitate in hexane and heptane, and it is soluble in toluene. The interface movement is observed for only four to five hours, asphaltene precipitation or solubility may take more than 24 hours to occur. Hence it is difficult to determine the influence of asphaltene precipitation or solubility, on diffusivity dependence on concentration. The test results proved that diffusivity displayed high concentration dependence (Crank and Park, 1968; Neogi, 1988; Crank, 1975).

2. INTRODUCTION

Heavy oil extraction offers challenges because of its high viscosity. One process introduces steam at high temperature and pressure over oil in the reservoir. The steam heats up the oil and the viscosity drops to 1 cp, which helps to bring up the oil to the surface which is the steam assisted gravity drainage (SAGD). In a related process n-hexane, n-heptane are used to treat the oil. They dilute the oil bringing down the viscosity. In addition, asphaltenes are precipitated which lowers the viscosity further. In a synthesis, C_6 – C_7 vapors are introduced instead of steam, and mass transfer into oil takes place. This is called the solvent vapor extraction (VAPEX) process. An overview of this area is presented by Banerjee (2012) and a quantitative description of VAPEX, but without mass transfer, has been given by Lin et al (2014). Although the solvents are introduced in vapor form, when dissolved in oil they acquire consistency of liquid state, that is, condensed phase (Prausnitz et al, 1999). This holds even when the solvent is a permanent gas. As a result in the work below liquid phase solvents are used to look at diffusivities of solvents in oil.

2.1.SELF-SHARPENING

We are interested here in quantifying the rate of dissolution of heavy oil in C_6, C_7 and toluene. A small amount of heavy oil is put in a test tube and a solvent is layered over it. Under conditions of no stirring, an interface is seen. The location of the interface moves with time till the solvent turns brown to black and nothing else can be observed. The question arises as to why an interface should exist when the oil and solvent are miscible. To answer this question (and subsequently) we assume that the heavy oil is very much like a polymer. In such a case a look at the rate of dissolution of polymer in a solvent also shows that an interface forms (Miller-Chou and Koenig, 2003) and stays for a long time.

There are explanations as to why this happens, but the one we are interested is in the role of concentration dependent diffusivity (Vrentas and Vrentas, 1998). The profile of penetrant entering the oil is sketched in Figure 2.1. If the diffusivity is concentration dependent

$$D = D_o e^{\alpha\phi} \tag{1}$$

where $\alpha\phi$ is positive and large ~ 5-15, α is defined in Equation. 1 and ϕ is the volume fraction of the penetrant. The regions of large concentrations will show higher fluxes than the region of lower concentrations which will show lower fluxes. This makes the profile become sharper as shown in Figure 2.2. An interface is now observable. For diffusivity given by Equation. 1, Neogi (1988) has obtained the profile which is shown in Figure 2.3 for $\alpha\phi$ = 15. It is important to note that ends do not matter in Figures 2.2 and 2.3 , but is all important in Figure 2.1. Thus, it is possible to use the results of Neogi (1988) for a membrane with a finite thickness to an infinite system in the contacting process described earlier.

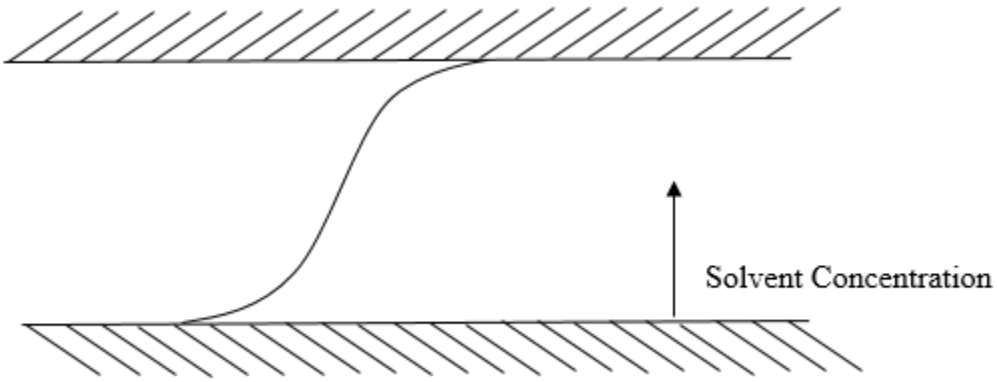

Figure 2.1. Schematics of penetrant entering the oil under diffusion when the diffusivity is a constant. The concentration profile is smooth.

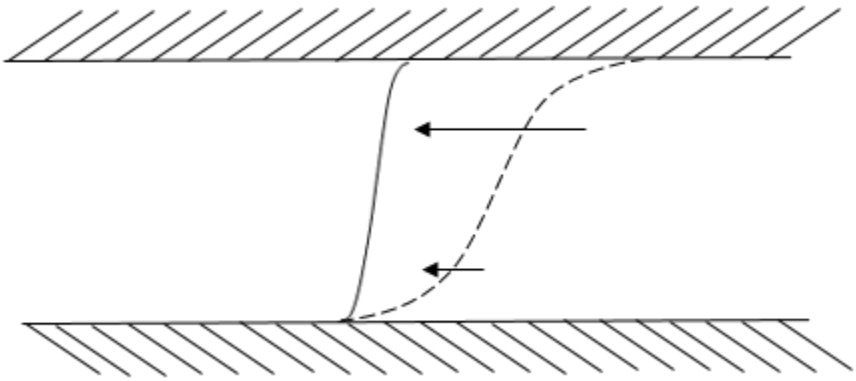

Figure 2.2. If the diffusivity is an increasing function of the solvent concentration then the region of the profile with higher concentration moves ahead much faster than the basic profile and the region of low concentration more slowly. The consequence is a buildup, also called self-sharpening.

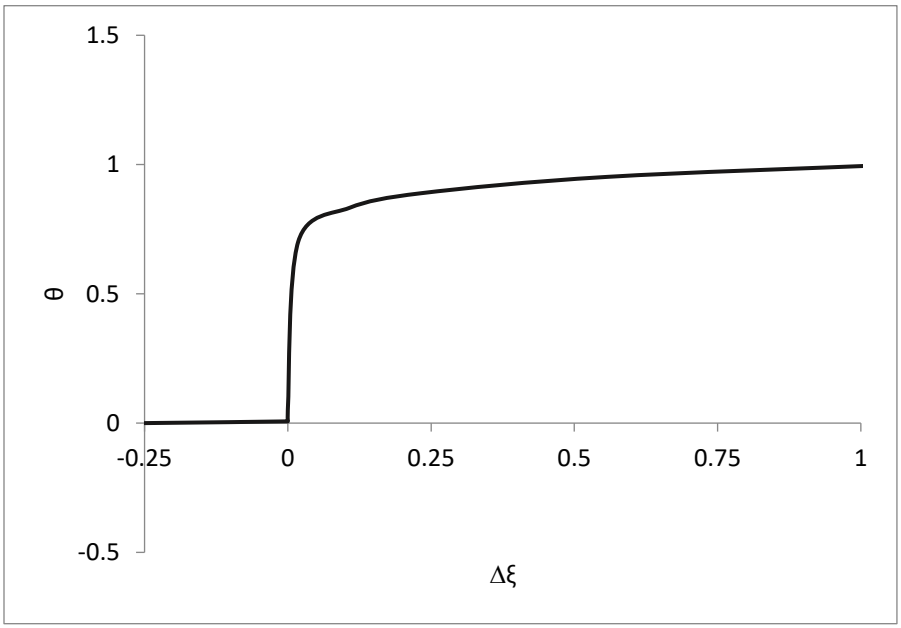

Figure 2.3. Neogi (1988)'s solution to Equations. 1 and 6 plotted in the form of dimensionless concentration, θ and dimensionless distance, $\Delta\xi$ from the interface for $\alpha\phi_{\infty}$ = 15. The foot of the profile is not discontinuous and it is easy to see where the interface between oil (black) and solvent (transparent) will be.

2.2. DIFFUSION COEFFICIENT, FLUX AND CONSERVATION EQUATION

The diffusivity of a penetrant in a polymer is given by free volume theory (Vrentas and Duda, 1979) as

$$D = RTA_d.\exp[-\frac{B_d}{f+(g-f)\phi}] \tag{2}$$

where A_d and B_d are constants, and B_d is the size of a hole that needs to be created for the penetrant to move into. The assumption here is that free volumes remain small to be rate controlling. The volume fraction of the penetrant is ϕ, and f and g are the free volume fractions of the polymer and the penetrant. Free volume is defined as the total volume less the volume occupied as represented with molecules of hard dimensions. The free volume fraction of a polymer f is small but that of small penetrant species g is large, as a result the free volume increases with solvent concentration and so does the diffusivity. Fujita (1961) has reviewed this area earlier and showed that other transport properties also follow the free volume theory. Tran et al (2012) fitted the data of Chung et al (1988) of a heavy oil – CO_2 system for a number of properties using free volume theory. The agreement was very good. Chung et al (1988) did not have the diffusivity data but Tran et al (2012) were able to predict the diffusivities and found them to be like Equation. 1. The conclusion was that f is larger in heavy oils than observed in polymers, thus $(g - f)$ is smaller. Expanding for small values of $(g - f).\phi$ inside the exponent by Taylor series in Equation. 2, we get

$$D = RTA_d.\exp[-\frac{B_d}{f}].\exp[\frac{B_d(g-f)\phi}{f^2}] \tag{3}$$

which corresponds to Equation. 1. Note that Equation. 3 shows α in Equation. 1 to be positive. It is also known that in polymers well over the glass transition temperature one

also has diffusivities that depend exponentially on the penetrant concentration (Prager and Long, 1951).

In the present case Figure 3.1 shows that the total volume of oil and solvent does not change with time. Consequently, we assume that the partial volumes of oil and water remain constant and same as those of pure components. In a one dimensional system, this has an important result that when we use volume average velocity to determine the fluxes, there is no convective term (Camacho and Brenner, 1995) that was otherwise expected (Slattery, 1972). The flux in the stationary coordinates is same as that given by Fick's law in moving coordinates

$$N_x = J_x \tag{4}$$

following notations in Bird, et al (2002). If a volume average velocity is used for Fick's law, it results in

$$J_x = -D\frac{\partial c}{\partial x} \tag{5}$$

exactly. This leads to conservation equation

$$\frac{\partial c}{\partial t} = -\frac{\partial N_x}{\partial x} = \frac{\partial}{\partial x} D \frac{\partial c}{\partial x} \tag{6}$$

When volumes are additive, the specific molar volume v^o remains a constant and same as that of the pure system. Hence multiplying Equation. 6 with v^o leads to

$$\frac{\partial \phi}{\partial t} = \frac{\partial}{\partial x} D \frac{\partial \phi}{\partial x} \tag{7}$$

We have taken time to develop the conservation equation in this system as discussions have become very contentious in this area (Ghanavati et al, 2014).

2.3. APPROXIMATE CONCENTRATION PROFILE OF THE SOLVENT

Solution to Equations. 1 and 7 when $\alpha\phi$ is large is difficult to obtain. Neogi (1988) assumed that $\alpha\phi_\infty = \bar{\alpha} = \ln\left|\frac{1}{\varepsilon}\right|$ where ϕ_∞ is the saturation volume fraction of the solvent and ε is a small quantity. When $\bar{\alpha}$ = 5, ε = 7x10^{-3} and when $\bar{\alpha}$ = 15, ε = 3x10^{-7}. Such an assumption led Neogi (1988) for the problem of diffusion in a membrane to an asymptotic solution for $\theta = \phi/\phi_\infty$ where the membrane initially has no solvent. The profile obtained is very sharp as shown in Figure 2.3 and rides on a pseudo-interface between the solvent-rich and solvent lean regions. Dimensionless quantity ξ_o was defined as current location of an interface in the membrane, dividing a region which is saturated by the solvent, θ = 1, from a region which is completely dry, θ = 0. The overall mass of solvent is conserved. In dimensional form

$$\Delta x_o = [\frac{2D_o e^{\alpha\phi_\infty} t}{\alpha\phi_\infty}]^{1/2} \tag{8}$$

where x_o is the dimensional ξ_o and Δx_o is the amount by which the interface has moved. Equation. 8 contains a problem in the limit α goes to zero. This is because it has been obtained under the condition that α is large. An empirical correction would be

$$\Delta x_o = [\frac{2D_o (e^{\alpha\phi_\infty} - 1)t}{\alpha\phi_\infty}]^{1/2} \tag{9}$$

where the exponential factor is much larger than 1 for large values of α. If the initial concentration of the solvent in oil is ϕ_o instead of zero, we get

$$\Delta x_o = [\frac{2D_o (e^{\alpha\phi_\infty} - 1)t}{\alpha(\phi_\infty - \phi_o)}]^{1/2} \tag{10}$$

where the above correction for small values of α has been made. In the present system $\phi_\infty = 1$.

When oil is contacted with a solvent some discussion is needed on how the above results can be applied. As shown in Figure 3.1 a visible interface or pseudo-interface is observed for a long time even though some mass transfer is going on as evidenced by the swelling of the oil phase. The oil phase is black and the solvent phase is transparent. It is also possible to define a mathematical interface with ϕ = 1 on one side and ϕ = 0 on the other such that the solvent material balance is satisfied $\int_0^L \phi dx = 1.(L - x_o) + 0.x_o$ where zero and L are the two boundaries. It is evident from Figure 2.3 that this mathematical interface will lie very close to the region where the solvent concentration changes very sharply, which is the region of visible interface. Thus, if the visual interface can be located by color change within a band of Δ in its location, then it can also be assumed that the mathematical interface x_o will lie there with an error of $\pm \Delta/2$. Then the above equations will apply. Thus, it is being assumed that the mathematical interface also lies in this band. At very large times not just this band becomes very large, the solvent becomes brown when it becomes difficult to identify the region of transition.

In desorption experiments, vacuum is pulled over oil containing solvent. The result for desorption is

$$\Delta x_1 = \left[2 \frac{e^{\hat{\alpha}}(e^{\hat{\alpha}} - 1)}{\hat{\alpha}} D_o t \right]^{1/2} \tag{11}$$

where x_1 is the location of the mathematical interface and $\hat{\alpha} = \alpha\phi_o$. However, both the interfaces, mathematical and pseudo-interface, between solvent rich ($\phi = \phi_o$) - solvent lean (ϕ = 0) regions, lie inside the oil which is black. Thus the visual interface cannot be observed. There is a third interface here, the liquid-vacuum interface. As the volumes are additive, the total change in volume leads to

$$\Delta x_i = \phi_o \Delta x_1 = \phi_o \left[2\frac{e^{\hat{\alpha}}(e^{\hat{\alpha}} - 1)}{\hat{\alpha}} D_o t \right]^{1/2} \tag{12}$$

where x_i here is the oil-vacuum interface, where 1 has been subtracted off to prevent singularity at $\hat{\alpha}$ = 0.

2.4. PRESENT EXPERIMENTS AND LITERATURE

Ghanavati et al (2014) have provided a review on a lot of data that have been reported on diffusivities of solvents in crude oil. The reasons why the results cannot be used or are not relevant to present purposes are varied and only some publications are described below. Guerrero et al (2008) and Afshai and Kantzas (2007) consistently fit their data to an expected profile using constant diffusivity. They also neglect the convective term, assume no swelling, and interpolate to get diffusivity as a function of concentrations, using spatially averaged concentration in the unsteady state case as the above concentration. As mentioned earlier, we are aware that all these assumptions produce errors, although, it is not clear by how much. Both our formulation and experiments avoid these problems. Fadei, Shaw and Swinton (2013) actually measure the concentration profile when heavy oil is contacted with toluene over microscopic distances. They do not include convection, and back calculate the diffusivity from the partial differential equation

that has no convective term, and use mass fractions. They use light absorption to calculate the solvent concentration but cannot process deep into the oil side because it is all black there. Their results range from toluene mass fraction of 0.1 to 0.9 and diffusivities of $0.5x10^{-5}$ to $3x10^{-5}$ cm^2/s. The diffusivity values are quite high and concentrations do not approach zero concentration well. Similar results are seen for pentane in heavy oil (Zhang et al, 2007) where x-ray absorption is used instead of visible light. The diffusion data as a function of mass fraction of pentane are concave upwards instead of convex upwards as in case of toluene. In the VAPEX process the solvent enters the region occupied by heavy oil and the leading edge ends at zero solvent concentration. This is where the diffusion coefficient is expected to be far lower and control the rate of penetration into the oil.

The present scheme takes into account that it is very difficult to see inside black oil and utilizes the fact that the oil-solvent junction will be sharp. Vrentas and Duda (1979) discuss diffusivity data of ethylbenzene in polystyrene that show that the diffusivities fall from $5x10^{-7}$ to 10^{-9} cm^2/s when the solvent concentration falls from 0.1 mass fraction to zero. The lowest diffusivity found in the above experiments is 10^{-7} cm^2/s by Afshai and Kantzas (2007). It is reasonable to suggest that the diffusivity of a solvent in heavy oil behaves in the same way as that in dry polymer. It has been observed earlier that the properties of heavy oil-solvent system follows the free volume model (Tran et al, 2012). The free volume theory predicts the sharp fall in diffusivities at low concentrations. Strong concentration dependence at low solvent concentrations implies a very large concentration sharpening as seen in Figure 2.3. In addition, the mixing zone is also very small and the amount of oil there will be low. The details of the above development in form of solution Equations. 1 and 7 for large values of α are given in Appendix A. The experiments below

where a liquid solvent is layered on the heavy oil and the interface is tracked with time, provides a very simple way to obtain concentration dependent diffusivities, because the solution to the boundary value problem is known. Because the encroaching solvent front is led by a region of very low solvent concentration, it is this speed that is rate controlling. We can hence simplify measurements by tracking the speed of the front and not the concentration distribution in boundary layer. This novel method is attempted below for the first time. The dissolution experiments give us one number for two constants D_o and α and it is expected that a desorption experiment will provide another number allowing us to calculate the two constants. Because the nature of heavy oil and solvent are not accounted for, the D_o and α pair are unique to a solvent-heavy oil pair. For completion, it is note that as the free volume becomes large at large solvent volume fractions ϕ, neither Equation. 2 nor Equation. 1 are valid.

3. EXPERIMENTAL

Heavy oil from A Hauser, Kansas, was used below. Brookfield viscometer was used to measure the viscosity of 4253 mPa.s (cp) at room temperature (~ 23ºC) and API gravity was found to be 19.9º (specific gravity of 0.934) and 929.8 mPa.s at 50 ºC and an API gravity of 21.9º (sp.gr. 0.9224). See Table 3.1. Solvents, *n*-hexane, *n*-heptane and toluene were purchased from Sigma Aldrich and used as received.

Table 3.1. Properties of oil

	Room Temperature (23 ºC)	30 ºC	40 ºC	50 ºC
Viscosity mPa.s (cP)	4253	1884	1206	929.8
API gravity/ sp.gr	19.9º/0.9340			21.9º/0.9224

Oil was first preheated to 90 ºC in a water bath and then poured into a test tube in the water bath as oil at 90 ºC flowed more easily. The test tube was held in a metal holder in the water bath which was checked to be vertical. The bath temperature was then brought down to 30 ºC. Solvent, preheated to 30 ºC was then very gently poured on the oil when it reached 30 ºC. We have performed such experiments earlier where one aqueous solution was contacted with another or with a low viscosity oil, where the layering process was very difficult. The upper liquid was layered over the lower liquid over a long time using a micropipette (Williams et al, 1999). However, it was much easier here because the heavy

oil is very viscous and damped disturbances well. Only a metered pipette was used to layer the top liquid on the glass walls to dampen the flow. Upon addition of solvent on oil, the solvent appeared to be immiscible with the oil and an interface was formed which remained clear and easy to track as seen in Figure 3.1. The initial height of the solvent interface was noted and the test tube was sealed. Every hour the test tube was removed from the water bath and a photograph taken. Figure 3.1 actually shows a series of photographs of a same system. Individual photographs were enlarged as shown in Figure 3.2 for hexane on oil at 30 ºC at 4 hours. The curvature observed in the oil profiles were in large part due to the curvature of the glass tube of 10.99 mm inside diameter.

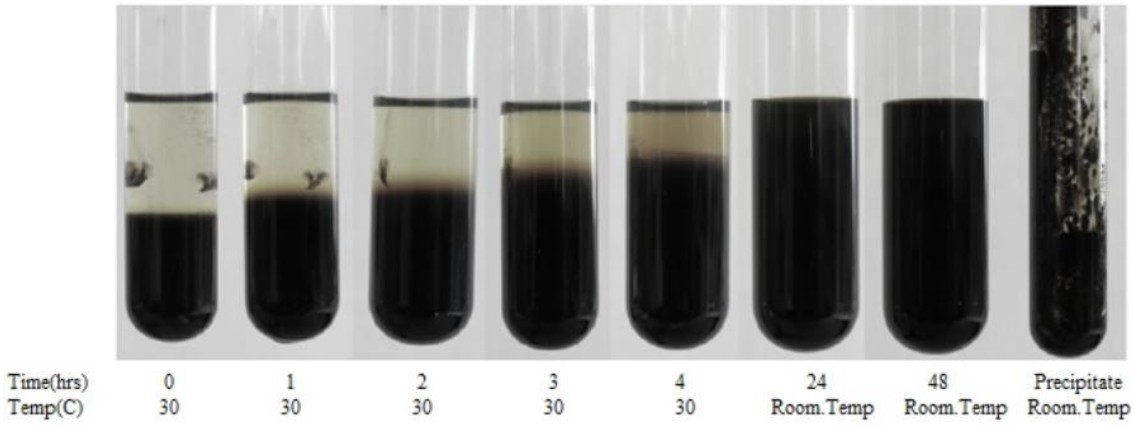

Figure 3.1. Interface between heavy oil and solvent, hexane, from 0 to 4 hours at 30 ºC. Solvent interface height decreases with time. The sample was allowed to rest for 48 hours at room temperature and diluted oil was poured out to reveal asphaltene precipitation on the sides of the test tube.

The interfacial region was obtained by scanning horizontally from top and going down until a position was found that was all black over the full cross-section: that is the

lower line in Figure 3.2. Another attempt was stopped where the color was not black over the entire cross-section. The difference was 0.4 mm and hence the mathematical interface located midway had an error of ± 0.2 mm. The errors were determined for each case. The two lines in Figure 3.2 were cut in half to aid viewing here. With care, the error can be halved to ± 0.1 mm, but not always.

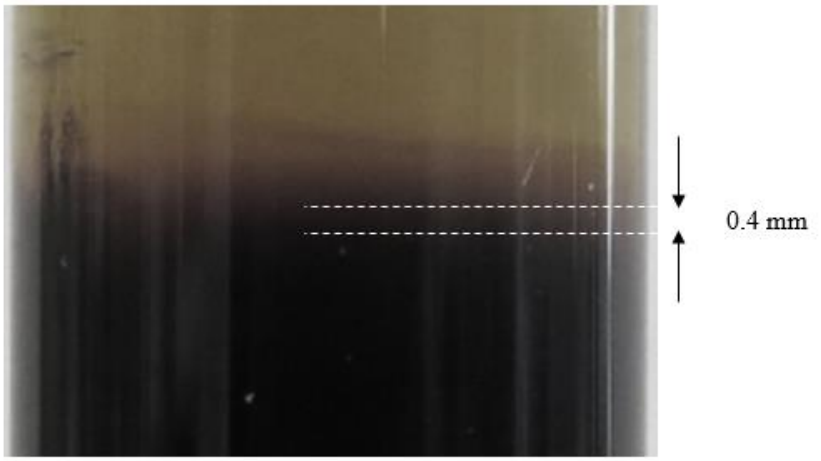

Figure 3.2. Enlarged portion from a heavy oil-hexane sample at 4 hours showing the interfacial region. Interface is not of zero thickness, but about 0.4 mm thick.

Measurements were discontinued in 3-4 hours beyond which the interface became difficult to identify. At 5 hours, the interface became quite fuzzy and the experiment was discontinued with bath temperature allowed to return to room temperature. Pictures were taken 24 and 48 hours later as shown, where the solution was fully equilibrated. At 48 hours, the liquid was drained out and showed the asphaltene precipitate adhering to the sides. All of the above description covers the full panel of photographs in Figure 3.1.

These experiments were carried out for hexane, heptane and toluene at 30º, 40º and 50 ºC. Toluene becomes dark too easily at higher temperatures. Although we took care to satisfy the accuracy maintained here, the error in this case is expected to be more. One other system that was analyzed, was 80 vol.% oil and 20 vol.% heptane (or hexane) which was contacted with heptane (or hexane) at 50 ºC.

Desorption experiments were very difficult to carry out. First of all, it made no difference if a vacuum was pulled over the mixture or if the mixture was allowed to evaporate in air. It suggests that the mass transfer resistance in the liquid phase was just too high that the two cases gave the same result, which is that the solvent concentration at the interface is always zero. Secondly, desorption was very slow for heptane and toluene so that only the experiments at high temperature, 50 ºC were conducted. Since hexane was more volatile, desorption experiments were studied at the lower temperatures of 30 and 40 ºC as well. Further, to stop the oil from clinging to the sides as the interface receded, we rinsed the inside of the tube with polydimethyl siloxane first, which made the walls non-wetting to oil. Finally, in spite of all these steps, the interface looked slightly bowed. The numbers for the liquid level were all collected at the center of the tube where the interface was the lowest.

4. RESULTS AND DISCUSSION

The viscosities and some specific gravities are shown in Table 3.1. The heights of the interfaces with time for the three solvents are shown in Figure 4.1 and the changes in the location of the interfaces with square root of time are shown in Figure 4.2. The linear fits are very good.

To determine the effect of temperature on the decrease of solvent interface height with time, dissolution experiments of hexane, heptane and toluene in heavy oil were performed at two higher temperatures, 40 and 50 ^{o}C. The changes in the interface height at 30, 40 and 50 ^{o}C with square root of time are shown in Figure 4.3 for hexane, 4.4 for heptane and 4.5 for toluene. Toluene-oil sample turned too dark after 2 to 3 hours at higher temperatures. Again the fits are linear and agree well with Equation. 9. Asphaltene is insoluble in hexane, heptane but soluble in toluene (Guo et al, 2014; Nikolaides, 2015). Dissolution of solvents in heavy oil led to asphaltene precipitation in hexane and heptane in present experiments but not in toluene.

Shown in Figures 4.6 and 4.7 are the responses of hexane and heptane at 50 ^{o}C where the oil phase initially had solvents at $\phi_o = 0.2$. If we take the slope for hexane and heptane and divided with the slope for hexane and heptane when there is no solvent in oil present initially, we get 0.006/0.0049 = 1.22448 for hexane and 0.0043/0.0039 = 1.10256 for heptane. This ratio can be calculated from Equations. 8 and 9 to be 1.11803. The accumulated errors are 9% and 2.3% and show that the data and theory to be consistent and reliable to a high degree.

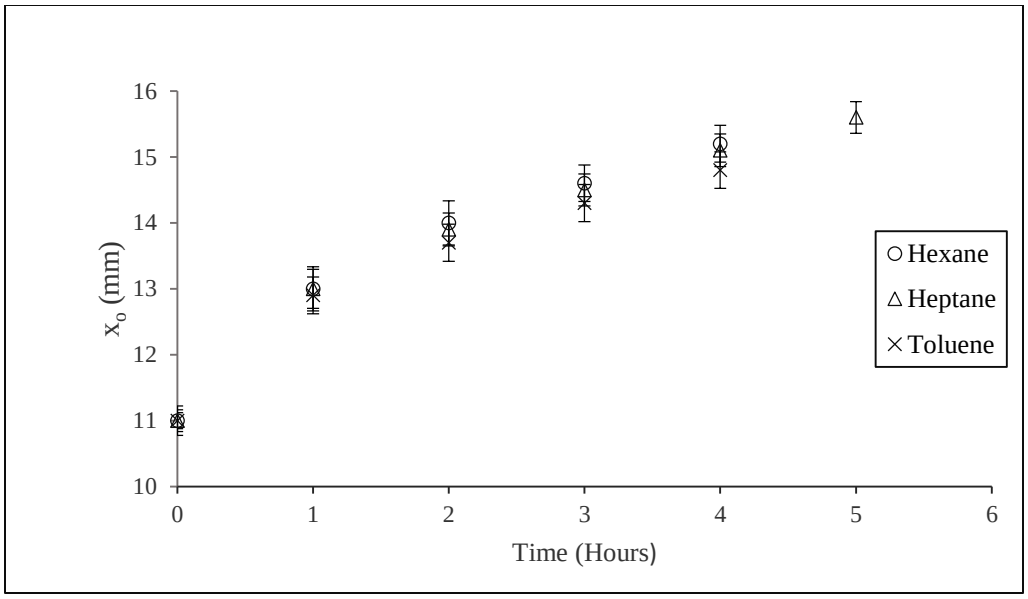

Figure 4.1. Location of the oil-solvent interface in dissolution of oil measured from the bottom, shown for hexane, heptane and toluene in heavy oil from 0 to 5 hours at 30ºC plotted as a function of time in hours. Error bars are shown.

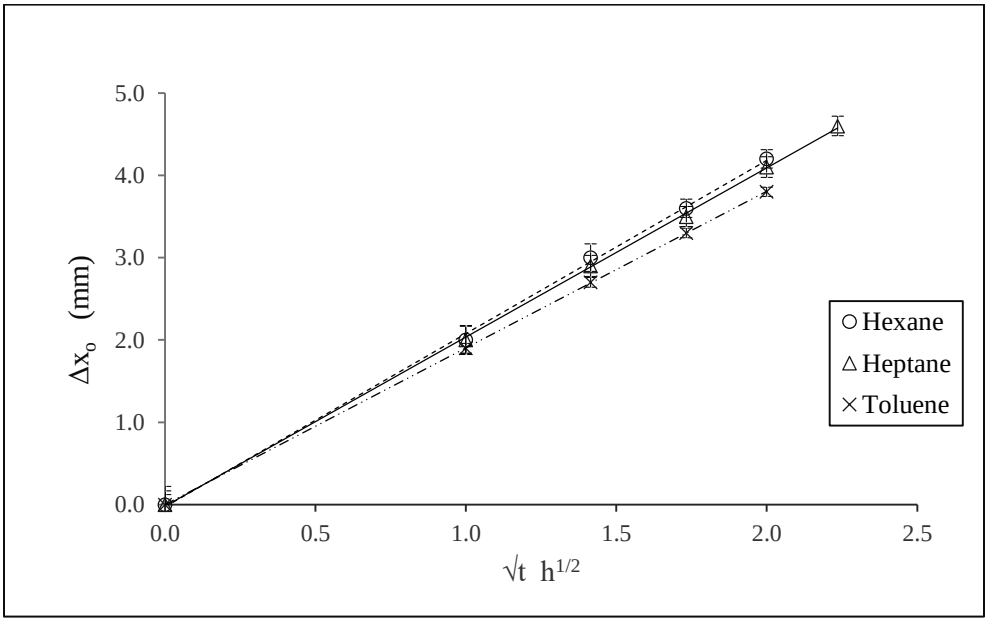

Figure 4.2. Experimental data fitted to theory in form of location of the interface for hexane, heptane and toluene in heavy oil at 30 ºC plotted versus $\sqrt{t}$ where time t is in hours. Error bars are shown. Circle for hexane, triangle for heptane and cross for toluene.

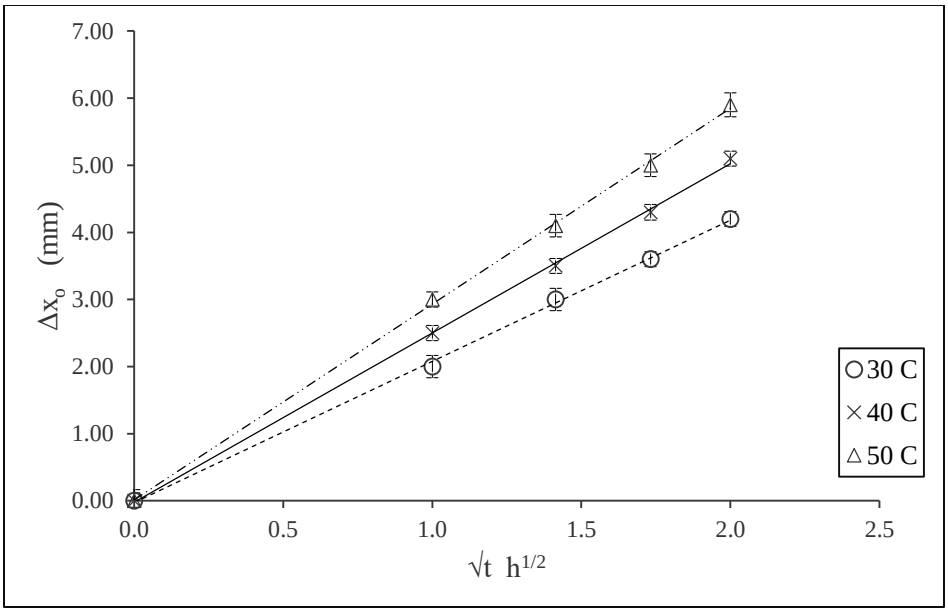

Figure 4.3. Experimental data fitted to theory in form of movement of the interface versus $\sqrt{t}$ are shown at 30º, 40º and 50ºC for hexane.

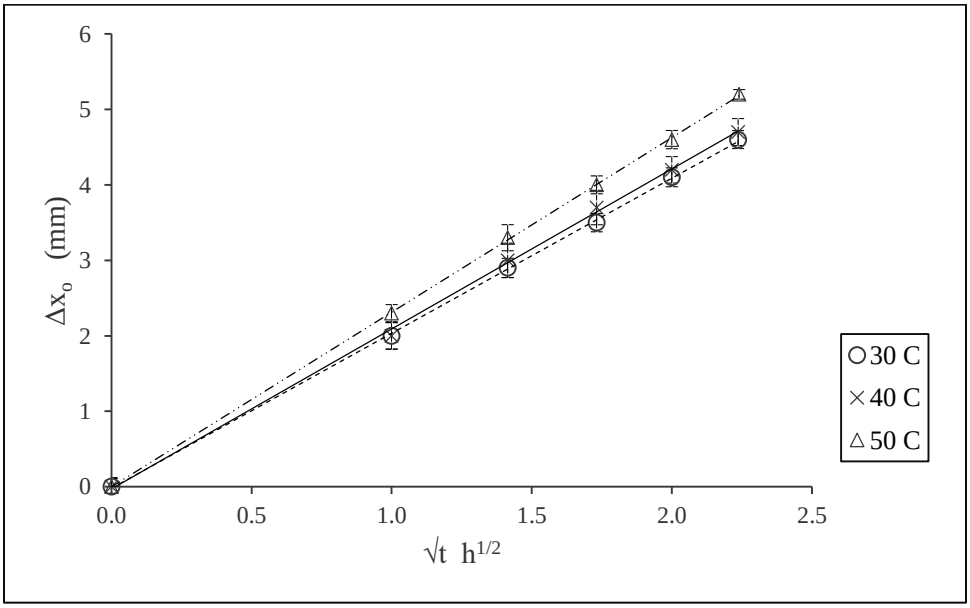

Figure 4.4. Experimental data fitted to theory in form of movement of the interface versus $\sqrt{t}$ are shown at 30º, 40º and 50ºC for heptane.

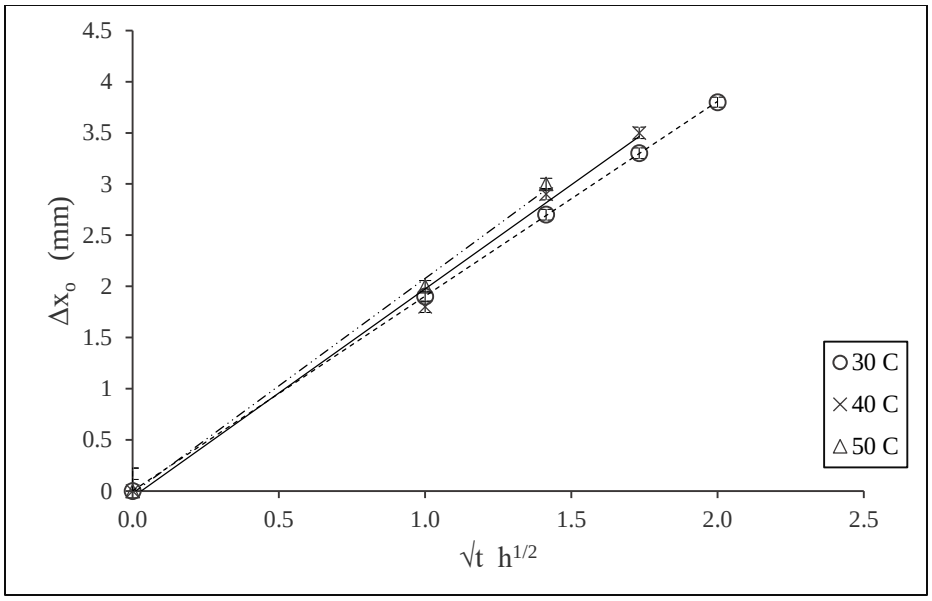

Figure 4.5. Experimental data fitted to theory in form of movement of the interface versus $\sqrt{t}$ are shown at 30º, 40º and 50ºC for toluene.

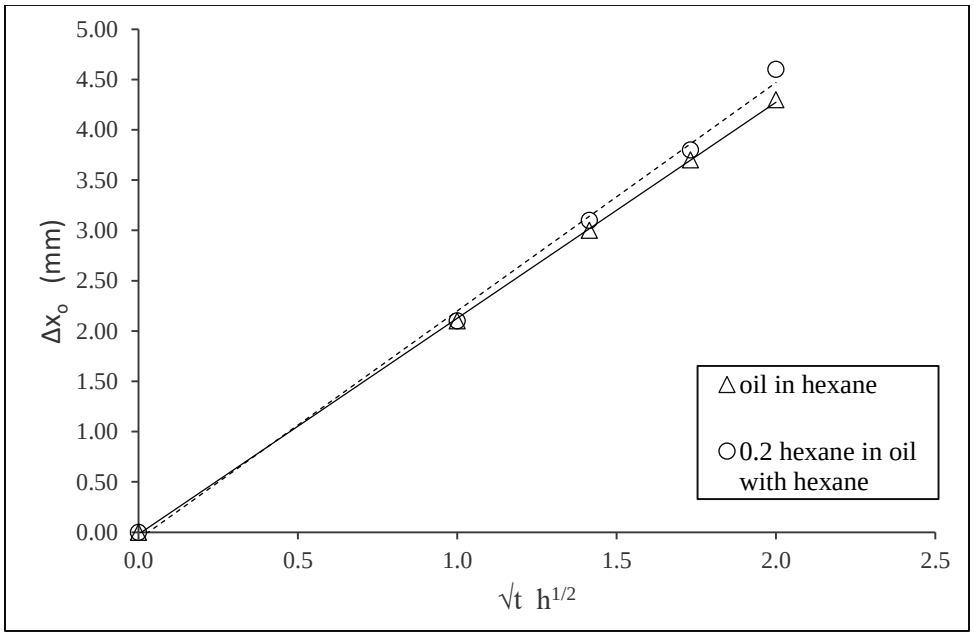

Figure 4.6. Experimental data fitted to theory in form of movement of the interface in dissolution of oil for pure oil in hexane and oil with 0.2 volume fraction hexane dissolving in pure hexane, both at 50ºC.

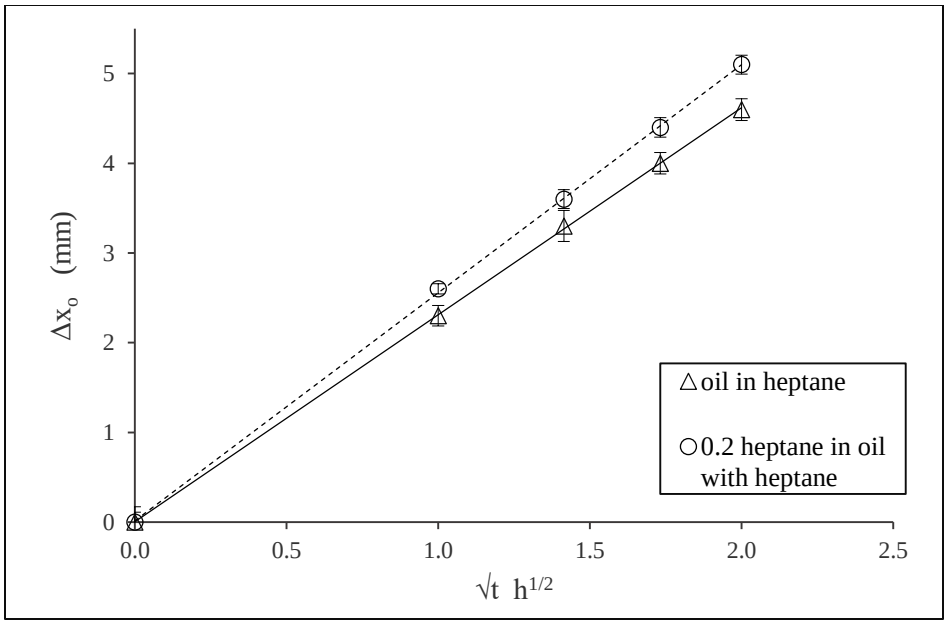

Figure 4.7. Experimental data fitted to theory in form of movement of the interface in dissolution of oil for pure oil in heptane and oil with 0.2 volume fraction heptane dissolving in pure heptane, both at 50ºC.

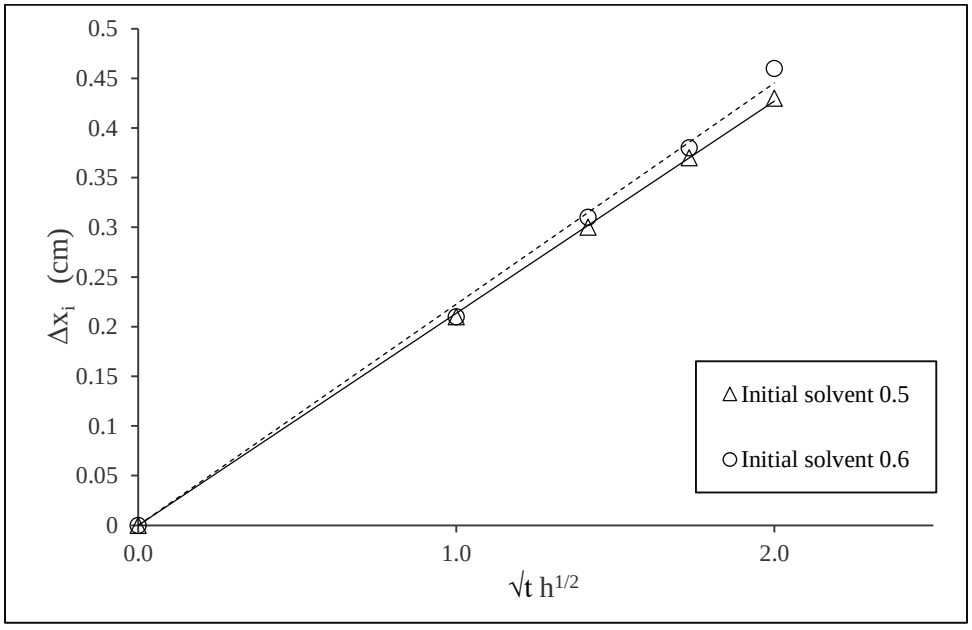

Figure 4.8. Experimental data fitted to theory for desorption at 50ºC of oil with 0.5 and 0.6 volume fraction hexane.

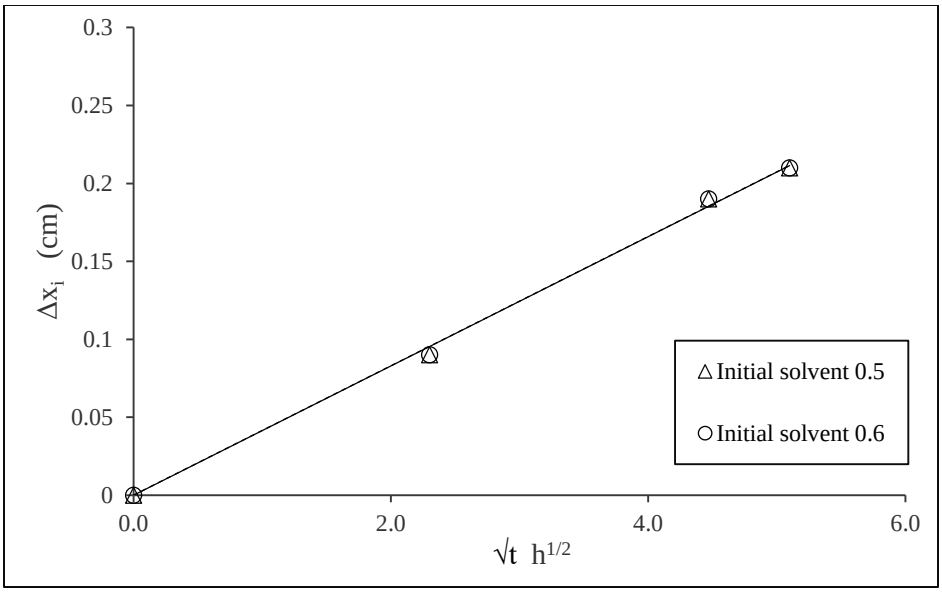

Figure 4.9. Experimental data fitted to theory for desorption at 50ºC of oil with 0.5 and 0.6 volume fraction heptane.

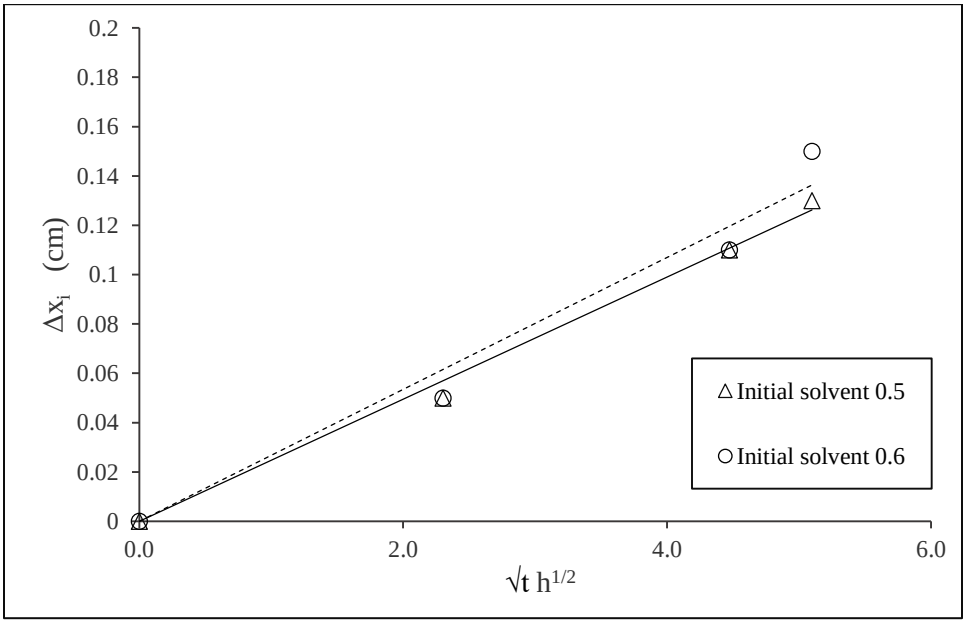

Figure 4.10. Experimental data fitted to theory for desorption at 50ºC of oil with 0.5 and 0.6 volume fraction toluene.

Desorption results at 50 ºC for ϕ_o = 0.5 and 0.6 for hexane in 4.8, heptane in 4.9 and toluene in 4.10. The slopes and what they represent are shown in Table 4.1 which also includes all our data.

Table 4.1. Summary of the slopes (from Figures 4.1-4.7 for dissolution and Figures 4.8-4.10 for desorption) from the data and their theoretical interpretation, Equations. 10 and 12).

ϕ_o	Temp	Dissolution		Desorption	
		0.0	0.2	0.5 (A)	0.6 (B)
n-hexane	30 ºC	3.5×10^{-3}		1.6×10^{-3}	1.7×10^{-3}
	40 ºC	4.2×10^{-3}		1.9×10^{-3}	1.9×10^{-3}
	50 ºC	4.9×10^{-3}	5.9×10^{-3}	3.6×10^{-3}	3.7×10^{-3}
n-heptane	30 ºC	3.4×10^{-3}			
	40 ºC	3.5×10^{-3}			
	50 ºC	3.9×10^{-3}	4.3×10^{-3}	7.6×10^{-4}	7.6×10^{-4}
toluene	30 ºC	3.2×10^{-3}			
	40 ºC	3.3×10^{-3}			
	50 ºC	3.5×10^{-3}		4.6×10^{-4}	4.6×10^{-4}

(A) Solvent added to oil to bring the solvent content to 0.5 volume fraction before desorption. (B) Solvent added to oil to bring solvent content to first 0.2 and homogenized and then more was added to bring it up to 0.6 before desorption

Many entries under desorption are missing which shows our limited ability to perform experiments of this kind. Nevertheless, we were able to check if the manner in which we make the samples had an effect. Between one dissolution data and one desorption data, at the same temperature and solvent, it should be possible to calculate D_o and α, but we were unable to obtain reasonable values. The diffusivity at infinite dilution can be calculated from Stokes-Einstein equation

$$D_o^{SE} = \frac{k_B T}{6\pi\mu_o a} \tag{13}$$

where k_B is the Boltzmann constant, μ_o is viscosity of the uncontaminated oil, and a is the radius of the solvent molecule which can be taken to be half of σ from Lennard-Jones potential (Bird et al, 2002). The calculated values of D_o using Stokes-Einstein equation are shown in Table 4.2. Vrentas and Duda (1979) indicate that over the temperature ranges used here, the diffusivities of ethylbenzene in polystyrene could even be lower than those in Table 4.2.

Table 4.2. Stokes-Einstein values for D_o Equation. 13.

T (^oC)	Temp (K)	Oil viscosity (g/cm·s)	Diffusivity (cm^2/s)		
			n-hexane	n-heptane	Toluene
30	303.15	18.84	3.77×10^{-9}	3.54×10^{-9}	3.98×10^{-9}
40	313.15	12.06	6.08×10^{-9}	5.71×10^{-9}	6.43×10^{-9}
50	323.15	9.298	8.13×10^{-9}	7.65×10^{-9}	8.60×10^{-9}

It is now possible to combine Stokes-Einstein values for Do, Table 4.2, with the values of the slopes (and their mathematical expressions) in Table 4.1, to calculate the values of α. These are shown in Table 4.3. It is seen that α values for dissolution are of the order of about 9 to 10. They decrease a little with increase in temperature, and do not change with the two cases of varying initial solvent concentrations in oil, volume fractions of 0.0 and 0.2. The values of α in desorption for n-hexane is of the order of 4 to 9 , that is, do not

agree with the dissolution values. However, the results from the two initial concentrations appear to agree. In general, α is independent of initial solvent concentrations and its values do show this feature. The experimental errors translate to ± 0.1 for α in dissolution at 95% confidence level except in case of toluene where it goes up to ± 0.5 to ± 1.5.

The fact that a dissolution-desorption pairs in Table 4.3 do not give acceptable values of the parameters most probably lies with high solvent concentrations used in the desorption studies. The free volume theory works only when the free volumes are low and restrict mobility. Heavy oil just about falls in this region in its free volumes. In presence of large amount of solvent, the free volume will become large will not be rate controlling and the free volume theory will not work. However, we could not run desorption experiments in the region of low values of ϕ_o.

Table 4.3. α values on combining data from Tables 4.1 and 4.2.

ϕ_o	Temp	Dissolution		Desorption	
		0.0	0.2	0.5 (A)	0.6 (B)
n-hexane	30 ºC	9.66 ± 0.12		8.85 ± 1.50	7.10 ± 1.11
	40 ºC	9.53 ± 0.10		8.51 ± 0.24	6.93 ± 0.72
	50 ºC	9.53 ± 0.10	9.72 ± 0.13	9.63 ± 0.05	7.79 ± 0.18
n-heptane	30 ºC	9.68 ± 0.05			
	40 ºC	9.21 ± 0.09			
	50 ºC	9.08 ± 0.03	9.04 ± 0.07	5.99 ± 0.29	4.64 ± 0.24
Toluene	30 ºC	9.37 ± 0.01			
	40 ºC	8.99 ± 0.54			
	50 ºC	8.73 ± 1.46		4.68 ± 0.51	3.74 ± 1.14

Since we have used a very low value of diffusivity at infinite dilution using Stokes-Einstein equation in desorption in particular, it would imply that it is correct if an average diffusivity $\bar{D}$ can be calculated for the desorption case. The rate at which the interface recedes is a moving boundary problem and a special case is that considered by Crank (1984) and given in Appendix B. The result for desorption is

$$\Delta x_i = \frac{-2\phi_o e^{-\frac{\left(\Delta x_i / t^{1/2}\right)^2}{4D_o}} \left(\frac{\bar{D}t}{\pi}\right)^{1/2}}{\lambda\left(1+erf\left(\frac{\Delta x_i / t^{1/2}}{(4\bar{D})^{1/2}}\right)\right)} \tag{14}$$

where $\lambda = \rho_o.v_o$, the density of oil ρ_o is interpolated from Table 3.1, and v_o the specific volumes of the solvents as functions of temperature are available in many data bases. Equation. 14 also shows that $\Delta x_i \propto t^{1/2}$. Values of the proportionality constants from the experimental data (slopes p) are taken from Table 4.1 and fitted to Equation. 14. (If we take $\Delta x_i / t^{1/2} = p$, then from Equation. 14 we get

$p = \frac{-2\phi_o e^{-\frac{p^2}{4D_o}} \left(\frac{\bar{D}}{\pi}\right)^{1/2}}{\lambda\left(1+erf\left(\frac{p}{(4\bar{D})^{1/2}}\right)\right)}$. These are solved to get $\bar{D}$ which are shown in Table 4.4. They are low compared to all the diffusivity data from previous work discussed earlier. This reinforces our basic premise that the diffusivities start from very low values at infinite dilution.

Table 4.4. $\bar{D}$ calculated using Equation. 14.

		Desorption $\bar{D}$ cm^2/s	
ϕ_o	Temp	0.5 (A)	0.6 (B)
n-hexane	30 ºC	3.05 x10^{-6}	3.10 x10^{-6}
	40 ºC	6.00 x10^{-6}	6.00 x10^{-6}
	50 ºC	9.70 x10^{-6}	9.70 x10^{-6}
n-heptane	30 ºC		
	40 ºC		
	50 ºC	6.00 x10^{-7}	6.00 x10^{-7}
Toluene	30 ºC		
	40 ºC		
	50 ºC	5.00 x10^{-7}	5.00 x10^{-7}

(A) Solvent added to oil to bring the solvent content to 0.5 volume fraction before desorption. (B) Solvent added to oil to bring solvent content to first 0.2 and homogenized and then more was added to bring it up to 0.6 before desorption

Overall, it appears that the diffusivity of these solvents is strongly concentration dependent, and in particular follows Equation. 1. However, we encountered a problem that desorption was the experimental method of choice for determining in particular the diffusivity at infinite dilution. It only worked partially, although it showed that the assumed concentration dependence was correct. It is possible to measure diffusivity at infinite dilution separately (Cussler, 2009), but it requires a different a separate system and has not been attempted here. We have not found any effect on diffusion from asphaltene precipitation and have inferred that asphaltenes take over a day to precipitate.

The large concentration dependence of the diffusivity has two implications. The first is that although we can perform oil recovery simulations using an effective constant diffusivity, in practice this effective value is very difficult to determine (Park, 1968). Second, complications result when numerical simulations are carried out using a strongly

concentration dependent diffusivity. It is prone to significant errors and stability problems (Ames, 1965).

5. CONCLUSIONS

The present method of measuring concentration dependent diffusivity is new and and is shown to work well. They are also consistent and accurate, showing good match with theory. However, it is not possible to get adequate data on desorption because of which either correlations have to be used for diffusivity at infinite dilution or other experiments need to be conducted to obtain this quantity. The data however show diffusivity to be strongly concentration dependent and the strong exponential dependence used here to be very suitable.

6. APPENDIX A

The derivations follow Neogi (1988) where a finite system has been changed to an infinite one.

Dissolution The development is based on the fact that the quantity ε, to be defined later, is small and hence $\ln\left|\frac{1}{\varepsilon}\right|$ is large but not very large. In particular, as $\varepsilon \to 0$, $\ln\left|\frac{1}{\varepsilon}\right| \to \infty$ but $\varepsilon^{v} \ln\left|\frac{1}{\varepsilon}\right| \to 0$ for all values of $v > 0$. Equation. 7 can be written as

$$\frac{\partial \theta}{\partial \tau} = \frac{\partial}{\partial x} e^{\bar{\alpha}\theta} \frac{\partial \theta}{\partial x} \tag{A-1}$$

where as $x \to -\infty, \theta \to 0$ and as $x \to +\infty, \theta \to 1$. Here $\theta = \phi/\phi_{\infty}$, $\tau = tD_{o}$ and $\bar{\alpha} = \alpha\phi_{\infty}$. Substituting $\bar{\alpha} = \ln\left|\frac{1}{\varepsilon}\right|, X = \frac{x - x_{o}(\tau)}{\omega}, \theta \sim \left[\ln\left|\frac{1}{\varepsilon}\right|\right]^{-1} \theta_{o} + \ldots$ we get

$$\frac{d\theta_{o}}{dX}.(-\omega).\frac{dx_{o}}{d\tau} = \frac{d}{dX}[e^{\theta_{o}} \frac{d\theta_{o}}{dX}] \tag{A-2}$$

Equation. A-2 is rewritten as

$$\frac{1}{1-A}\frac{d\theta_{o}}{dX} = \frac{d}{dX}[e^{\theta_{o}} \frac{d\theta_{o}}{dX}] \tag{A-3}$$

and

$$\frac{1}{1-A} = -\omega.\frac{dx_{o}}{d\tau} \tag{A-4}$$

where A is a constant. Here ω is small and goes to zero as $\varepsilon \to 0$. Equation. A-3 can be integrated twice subject to the boundary conditions $X \to -\infty, \theta_{o} \to 0, \frac{d\theta_{o}}{dX} \to 0$ to get

$$\frac{1}{x_o(0)-x_o(\tau)}.X = Ei(\theta_o) \tag{A-5}$$

where the condition $X \to +\infty, \theta \to 1$ is met approximately. *Ei* is the exponential integral, a special function. The rate law in Equation. A-4 now integrates to give

$$[x_o(0)-x_o]^2 = 2\tau/\omega \tag{A-6}$$

Now, the place where ω is introduced after Equation. A-1 shows ω to be thickness of the profile where θ falls rapidly from 1 to zero. Equation. A-4 also shows τ to be of the order of ω. So if we choose ω to be very small such as ε, then the profile falls very sharply, but stays for a very short time, which does not occur in practice. Thus, we increase the ω to be $\varepsilon \ln\left|\frac{1}{\varepsilon}\right|$ using the function of ε encountered earlier.

It is now possible to define x_o as equivalent to $\phi = 0 \quad \text{for } x < x_o$ and $\phi = \phi_\infty \quad \text{for } x \geq x_o$. It leads to a conservation rule that

$$\int_{x_o}^{\infty} (\phi - \phi_\infty) dx = 0 \tag{A-7}$$

Differentiating Equation. A-7 with τ, using Equation. A-1 and boundary conditions,

$$\frac{d}{d\tau}[x_o(0)-x_o(\tau)] = e^{\ln\frac{1}{\varepsilon}.\theta}.\left.\frac{\partial\theta}{\partial x}\right|_{x=x_o} \tag{A-8}$$

then using Equations. A-5, Equation. A-6 is obtained. In dimensional form, Equation. A-6 is

$$\Delta x_o = [\frac{2D_o e^{\alpha\phi_\infty} t}{\alpha\phi_\infty}]^{1/2} \tag{A-9}$$

and Equation. A-9 is Equation. 8 in the text.

Desorption In case of desorption set $\theta = 1 - \bar{\theta}$ in Equation. A-1, resulting in

$$\frac{\partial \bar{\theta}}{\partial \tau} = \frac{\partial}{\partial x} e^{\ln\frac{1}{\varepsilon}} . e^{-\ln\frac{1}{\varepsilon}.\bar{\theta}} \frac{\partial \bar{\theta}}{\partial x} \tag{A-10}$$

or

$$\frac{\partial \bar{\theta}}{\partial \tau} = \frac{1}{\varepsilon} \frac{\partial}{\partial x} e^{-\ln\frac{1}{\varepsilon}.\bar{\theta}} \frac{\partial \bar{\theta}}{\partial x} \tag{A-11}$$

where as $x \to -\infty, \bar{\theta} \to 0$ and as $x \to +\infty, \bar{\theta} \to 1$. Note for future reference, an extra ε on the right hand side in Equation. A-11. With $\bar{\alpha} = \ln\left|\frac{1}{\varepsilon}\right|, X = \frac{x - x_o(\tau)}{\omega}, \bar{\theta} \sim \left[\ln\left|\frac{1}{\varepsilon}\right|\right]^{-1} \theta_o + \ldots$ and using the same procedure as above,

$$\frac{1}{x_o(0) - x_o(\tau)} . X = E_1(\theta_o) \tag{A-12}$$

$$[x_o(0) - x_o]^2 = 2\tau / (\varepsilon\omega) \tag{A-13}$$

Equation. A-13 in dimensional form is given in Equation. 11. Note that in Neogi (1988), the extra ε is moved to the profile Equation. A-12 and the rate law Equation. A-13 is consequently modified. However, that makes the change in the concentration in the profile less steep. As a result, the ε has been moved to the rate law and as a result, the time over which Equation. A-13 applies is considerably shortened. that is, τ is of the order of $\varepsilon\omega = \varepsilon^2 \ln\left|\frac{1}{\varepsilon}\right|$. Other possible forms for ω could not be used.

7. APPENDIX B

The derivation below follows Crank (1984). The governing equation, Equation. 7 becomes

$$\frac{\partial \phi}{\partial t} = \bar{D}\frac{\partial^2 \phi}{\partial x^2} \tag{B-1}$$

Subject to the boundary conditions that as $x \to -\infty$, $\phi \to \phi_o$ and at $x = x_o$ $\phi = 0$. The jump mass balance is $\dot{m} = \rho(0 - \frac{dx_o}{dt}) = c(0 - \frac{dx_o}{dt}) - \bar{D}\frac{\partial c}{\partial x}$ at the interface. Here $\dot{m}$ is the solvent transferred across the interface (since oil is non-volatile), and ρ is the total density at the interface. Since the solvent concentration at the interface is zero, $\rho = \rho_0$ the density of pure oil at that temperature. The rest follows Crank (1984): error functions solution and the boundary conditions yield both the constants of integration and the location of the boundary.

In desorption experiments, solvents were allowed to evaporate. The result for desorption is

$$\Delta x_i = \frac{-2\phi_o e^{-\frac{\left(\Delta x_i / \sqrt{t}\right)^2}{4D_o}} \left(\frac{\bar{D}t}{\pi}\right)^{1/2}}{\lambda\left(1 + erf\left(\frac{\Delta x_i / \sqrt{t}}{\sqrt{4\bar{D}}}\right)\right)} \tag{B-2}$$

where x_i here is the visible oil-vacuum interface and λ corresponds to the product of density of oil and specific volume of solvent. More importantly $\Delta x_i = -p\sqrt{t}$ where p is a constant. Equation. B-2 is Equation. 14.

REFERENCES

Ames, W.F. (1965) Nonlinear Partial Differential Equations in Engineering, Academic Press, New York, p. 320.

Afsahi, B., and Kantzas, A. (2007) Advances in diffusivity measurement of solvents in oil sands, Journal of Canadian Petroleum Technology. 46, 56-61.

Banerjee, D.K. (2012) Oil Sands, Heavy Oil and Bitumen From Recovery to Refinery, PennWell Corp, Tulsa, p. 65.

Bird, R.B., Stewart, W.E., and Lightfoot, E.N. (2002) Transport Phenomena, 2nd edition., John Wiley, New York, p.536.

Camacho, J., and Brenner, H. (1995) On convection induced by molecular diffusion, IECRes, 34, 3326-3335.

Chung, F.T.H., Jones, R.A., and Nguyen, H.T. (1988) Measurements and the correlations of the physical properties of CO_2/heavy-crude-oil mixtures, SPE Reservoir Engineering, 3, 822 –828.

Crank, J. (1975) The Mathematics of Diffusion, 2nd edition, Oxford University Press, London.

Crank, J. (1984) Free and Moving Boundary Problem, Oxford Science Pub, Oxford, p. 102.

Cussler, E.L. (2009) Diffusion Mass Transfer in Fluid Systems. 3rd edition, Cambridge, p. 85.

Fedai, H., Shaw, J.M., and Swinton, D. (2013) Bitumen-toluene mutual diffusion coefficients using microfluidics, Energy & Fuels, 27, 2042-2048.

Fujita, H. (1961) Diffusion in polymer-solvent systems, Advanced Polymer Science, 3, 1-47.

Ghanavati, M., Hassanzadeh, H., and Abedi, J. (2014) Critical review of mutual diffusion coefficient measurements for liquid solvents+bitumen/heavy oil mixtures, Canadian Journal of Chemical Engineering, 92, 1455-1466.

Guerrero-Aconcha, U., Salama, D., and Kantzas, A. (2008) Diffusion coefficient of n-alkanes in heavy oil. Paper presented at 2008 SPE Annual Technical Conference, Denver, Colorado, SPE 115346.

Guo. B., Song. S., Ghalambor. A., and Lin. T.R. (2014) Offshore Pipelines: Design, Installation and Maintenance. 2nd edition, Elsevier, UK, p. 199.

Lin, L., Zeng, F., and Gu, Y. (2014) A circular solvent chamber model for simulating VAPEX heavy oil recovery process, Journal of Petroleum Science and Engineering, 118, 27-39.

Miller-Chou, B.A., and Koenig, J.L.(2003) A review of polymer dissolution, Progress In Polymer Science, 28, 1223-1270.

Neogi, P. (1988) Nonlinear elastodiffusion at small deformations in polymer membranes, Chemical Engineering Communications, 68, 185-195.

Nikolaides. A. (2015) Highway Engineering: Pavements, Material and Control of Quality. CRC Press, Boca Raton, p. 110.

Park, G.S. (1968) Methods of measurements, in Diffusion in Polymers, J. Crank and G.S. Park, eds., Academic Press, New York, p.1.

Prager, S., and Long, L.A. (1951) Diffusion of hydrocarbons in polyisobutylene, Joural of American Chemical Society, 73, 4072-4075.

Prausnitz, J.M., Lichtenthaler, R.N., and De Azevedo, E.G. (1999) Molecular Thermodynamics of Fluid Phase Equilibrium, 3rd ed, Prentice -Hall, New Jersey, p. 607.

Slattery.J.C. (1972) Momentum, Energy and Mass Transfer in Continua, 2nd edition, McGraw-Hill Book Co, p.18.

Tran, T., Neogi, P., and Bai, B. (2012) Free volume estimates of transport and thermodynamic properties of heavy oils with CO_2, Chemical Engineering Science, 80,100-108.

Vrentas, J.S., and Duda, J. L. (1979) Molecular diffusion in polymer solutions, American Institute of Chemical Engineering Journal, 25, 1-24.

Vrentas, J.S., and Vrentas, C.M. (1998) Dissolution of rubbery and glassy polymers, Journal of Polymer Science Part B: Polymer Physics, 36, 2607 – 2614.

Williams, C.L., Bhakta, A.R., and Neogi, P. (1999) Mass transfer in of a solubilizate in a micellar solution and across an interface, The Journal of Physical Chemistry B, 102, 3242-3249.

Zhang, X., Fulem, M., and Shaw, J.M. (2007) Liquid-phase mutual diffusion coefficients for Athabasca bitumen + pentane mixtures. Journal of Chemical and Engineering Data, 52, 691-694.

III. REVISITING BUTLER-MOKRYS MODEL FOR VAPEX PROCESS

Vijitha Mohan,[1] Parthasakha Neogi[1] and Baojun Bai[2]

[1] Chemical and Biochemical Engineering,

[2] Geosciences and Geological and Petroleum Engineering,

Missouri University of Science and Technology, Rolla, MO 65409-1230, USA

ABSTRACT

Dynamics of a process where a solvent in form of a vapor or gas is introduced in a heavy oil reservoir, is considered. The process is called the solvent vapor extraction process (VAPEX). When the vapor dissolves in the oil it reduces its viscosity, allowing it to flow under gravity and be collected at the bottom producer well. The conservation of species equation is analyzed to get a more appropriate equation to solve to get a concentration profile of the solvent in oil. In that, we disagree with an earlier model where the concentration profile is assumed. However, the final result provides the rate at which oil is collected which agrees with previous model in that it is proportional to $\sqrt{h}$ where h is the depth of the reservoir. A great deal of increase in output is seen if the oil viscosity decreases in presence of the solvent although the penetration of solvent into oil is reduced because under such conditions the diffusivity would decrease with decreasing solvent. One other important feature we observe is that when the viscosity reducing effect is very large, the recovered fluid is mainly solvent. Apparently, some optimum exists. Finally, the present approach also allows us to show how the oil-vapor interface evolves with time,

include the effects of reservoir heterogeneity and asphaltene precipitation using the existing framework, but have not been carried out because the length of computation and approximate nature of results.

NOMENCLATURE

Symbol	Description
C	solvent concentration in the liquid
D	diffusivity
D_o	diffusivity at infinite dilution
g	acceleration due to gravity
h	total height of the system
k	permeability
$\dot{m}$	solvent mass transfer rate
$P*$	a point on the interface, see Figure 5.1
q_b	solvent loss
$Q_b^{'}$	flow rate in the ribbon tangential to the interface
u	dimensionless boundary layer thickness, defined in Equation. 13
U	velocity in normal direction
V_p	velocity in tangential direction
v_L	specific volume of pure solvent dissolved in oil
$x*$	coordinate of point *P**
$z*$	coordinate of point *P**

α	concentration dependence term
δ	thickness of the boundary layer
η	coordinate in the tangential direction
$\Delta\rho$	density difference between oil phase and the gas phase
μ	viscosity
μ_o	viscosity at infinite dilution
ξ	coordinates in normal direction
ρ	total density
ρ_o	density of pure oil
ρ_{sL}	density of pure solvent dissolved in oil
ρ_{sV}	density of pure solvent in vapor form
σ	interfacial velocity normal to the interface
ϕ	volume fraction of solvent
ϕ_e	exit volume fraction
$\phi_{\min}$	solvent volume fraction on the inner edge of the ribbon
ϕ_o	initial volume fraction of solvent

1. PROLOGUE

As reported in the previous studies, solvent solubilized and moved through diffusion in heavy oil. Diffusion of solvents being highly dependent on the concertation of solvents used, there has to be an optimum solvent for solvent induced heavy oil recovery process. In this study a model to predict an optimum solvent, is created by revisiting an existing model by Butler and Mokrys (1989) for vaporized extraction (VAPEX) process. The solvent in vapor form is introduced through horizontal well. It dissolves and diffuses into the crude oil. The oil is now less viscous and drains under gravity into the production well. Butler and Mokrys (1989) used a two dimensional porous medium to simulate VAPEX process and predicted that the drainage rate of bitumen to be proportional to the square root of the drainage height. In this study, concentration dependence is introduced to derive the drainage rate of bitumen. It is found that concentration dependence of solvents influenced the penetration of solvent in bitumen and bitumen drainage rate. Higher concentration dependence caused lower penetration of solvent in bitumen but greater bitumen drainage which is saturated with solvent. Lower concentration dependence caused higher penetration of solvent and lower bitumen drainage. The influence of asphaltene precipitation on drainage rate is hard to determine. Concentration dependence did not have any effect on the shape of the solvent bitumen interface.

2. INTRODUCTION

Heavy crude has a very high viscosity making it difficult to extract the crude from the underground reservoirs. One method has been to use steam to heat up the oil when the oil viscosity drops to 1 cp and drains out under gravity. This is the steam assisted gravity drainage (SAGD). In another process a solvent in vapor form is used. Dissolution of the vapor into oil lowers the oil viscosity and in addition precipitates asphaltenes with further decrease in viscosity. This is the solvent vapor extraction process (VAPEX) (Banerjee, 2012). The solvent used can be vapors of C_7 and lower hydrocarbons and includes CO_2. In case of CO_2, the process can be used for CO_2 sequestration as well. Some oil that is recovered can be used to pay for the process provided not too much of CO_2 is lost alongside (Shaw and Bachu, 2002; Bachu and Shaw, 2003). The state of solvent in oil in all cases is liquid-like or saturated liquid when it applies.

The process that uses two horizontal wells is shown schematically in Figure 2.1. The top well is the injection well and the bottom well picks up the drainage. Butler and Mokrys (1989) were the first to quantify oil recovery which we have reworked here. They used a vertically held Hele-Shaw cell and introduced the vapor from the sides and collected the drainage at the bottom left corner shown in Figure 2.2. From the rate of collection, they were able to verify that the dependence on time and permeability from their model were correct. The fact that some hydrocarbons precipitate asphaltenes has been long known (Burke et al, 1990) and an organized view of precipitation thermodynamics also exists (Nhiem and Coombe, 1997). From a practical point of view, the precipitate plugs the well-bore area and discourses on what to do to relieve it also exist (Haghighat and Maini, 2010).

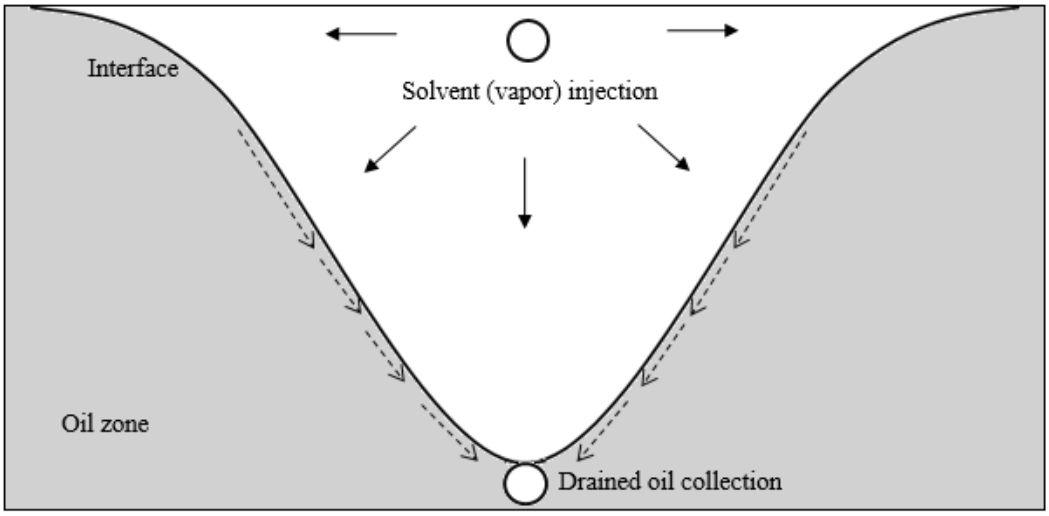

Figure 2.1. Schematic representation of VAPEX process using two horizontal wells. Solvent injected from the top and drained oil collected from the bottom, Butler and Mokrys (1991).

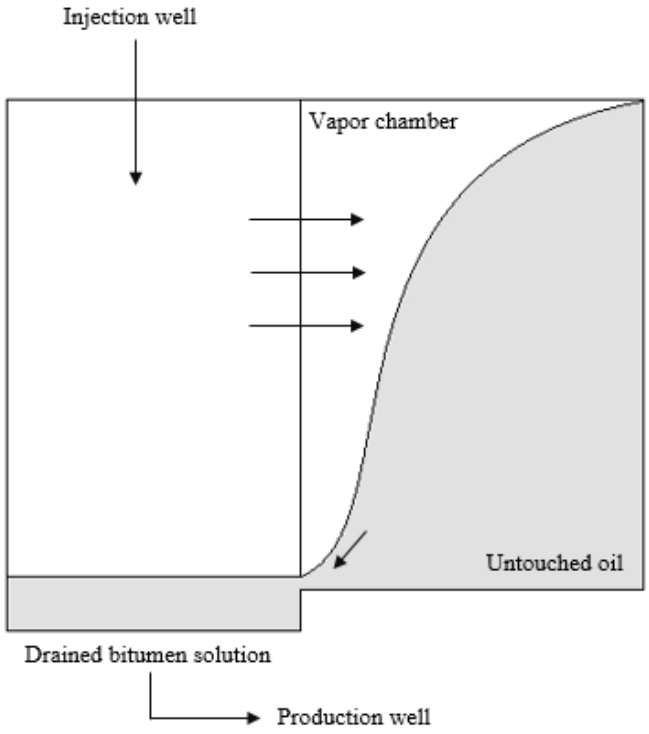

Figure 2.2. Schematic representation of VAPEX process in Hele-Shaw cell where solvent vapor introduced from sides into heavy oil and drained oil collected at the bottom, Butler and Mokrys (1989).

Below, we review Butler-Mokrys approach with emphasis on how the boundary value problem should be set up, and what the new solution is like. We then add to it a very simple model that includes oil precipitation in form of asphaltenes.

3. TRANSPORT MODEL AND ORDER OF MAGNITUDE ANALYSIS

Consider now Figure 3.1. If CO_2 is introduced as the solvent, then under reservoir conditions, CO_2 can be a gas or a liquid.

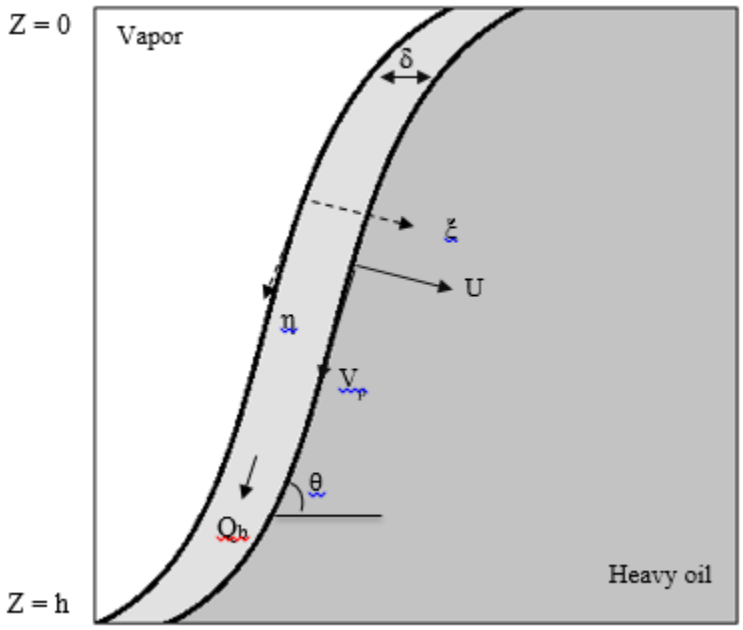

Figure 3.1. Cross sectional view of VAPEX process showing the region of vapor- heavy oil interaction, Butler and Mokrys (1989).

However, some experiments show that even at 5000 psi miscibility of CO_2 and heavy crude is not reached (Chung et al, 1988). For methane as a solvent, it would not liquefy under reservoir conditions. Consequently, for these two solvents, the boundary condition at the solvent-oil interface on the oil side is that the volume fraction of the solvent there is ϕ_o, a quantity dependent on the pressure in the solvent phase P. The pressure P can be taken to be a constant as the dissolution process is slow and the gas/vapor phase has comparatively very low viscosity. As a result, the pressure drop in the gas phase can be

neglected. In cases of C_2 and higher carbon numbers, the liquid form appears to be miscible with heavy oil, and $\phi_o = 1$. More details of such features are given by Mohan et al (2017a).

The transport aspects which have been under consideration by Butler and Mokrys (1989) and later in great details by Shi and Leung (2014) are taken up next using the approximations employed in boundary layer theory (Schlichting, 1968). If η and ξ are the coordinates in directions tangential and normal to the interface then the continuity equation can be written as

$$\frac{\partial \rho}{\partial t} + \frac{\partial \rho V_p}{\partial \eta} + \frac{\partial \rho U}{\partial \xi} = 0 \tag{1}$$

where V_p and U are the velocities in η (tangential direction) and ξ (normal direction). If the order of η is N the total length of the interface and of ξ is $\acute{o}$ the thickness of the interfacial region penetrated by the solvent, then it is expected that $N >> \acute{o}$ and $V_p >> U$. For constant ρ, the estimates in Equation. 1 become

$$\frac{V_p}{N} + \frac{U}{\delta}$$

If the two terms are comparable then boundary layer theory holds. However, the present case is somewhat different because the two velocities are related $V_p = \sin\theta . V_z$ and $U = \cos\theta . V_z$ and the angle θ is shown in Figure 3.1. Consequently, we also look at $\frac{V_p}{N} >> \frac{U}{\delta}$ or $\frac{V_p}{N} << \frac{U}{\delta}$. Both cases have been considered separately below. The momentum balance equation is replaced with Darcy's law

$$V_z = \frac{k\Delta\rho g}{\mu} \tag{2}$$

where z is the coordinate vertically downward. Further, $\Delta\rho$ is the difference between the local density and the density of the solvent and is hence zero in the solvent phase, g is the acceleration due to gravity and μ is the local viscosity. All of the driving force in Equation. 2 comes from gravity. In the oil phase not yet penetrated by the solvent, viscosity μ will be very high and hence V_z is practically zero there. Thus most of the flow is in the narrow interfacial region shown as a ribbon in Figure. 3.1 and in the direction tangential to the interface.

The conservation of the solvent in oil phase is given by

$$\frac{\partial\phi}{\partial t} + \frac{\partial V_p\phi}{\partial\eta} + \frac{\partial U\phi}{\partial\xi} = \frac{\partial}{\partial\eta} D\frac{\partial\phi}{\partial\eta} + \frac{\partial}{\partial\xi} D\frac{\partial\phi}{\partial\xi} \tag{3}$$

where the assumption that in the solution, the volumes are additive are made. D is the diffusivity. If the process is slow then term-by-term Equation. 3 approximates on neglecting the unsteady state term, as

$$\frac{V_P\phi_o}{N} + \frac{U\phi_o}{\delta} = D\frac{\phi_o}{N^2} + D\frac{\phi_o}{\delta^2}$$

The first term on the right hand side in above is negligible compared to the second and hence for the first case that $\frac{V_p}{N} >> \frac{U}{\delta}$ Equation. 3 becomes

$$\frac{\partial V_p\phi}{\partial\eta} = \frac{\partial}{\partial\xi} D\frac{\partial\phi}{\partial\xi} \tag{4}$$

which is similar to the boundary layer equation. However, if $\frac{V_p}{N} << \frac{U}{\delta}$

$$\frac{\partial U\phi}{\partial \xi} = \frac{\partial}{\partial \xi} D \frac{\partial \phi}{\partial \xi} \tag{5}$$

which is the equation governing concentration polarization. The unsteady state terms have been neglected in both Equations. 4 and 5 since the process is very slow. This is the quasi-static assumption and requires that down the line some correction is made that shows the unsteady nature of the process. We show subsequently how the interface changes with time.

In the next sections, Equations. 4 and 5 are solved with simple but realistic models for concentration dependence of D, μ and $\Delta\rho$ to obtain the rate at which oil is recovered, the results are compared to those by Butler and Mokrys (1989) and the limits of acceptability of the results are considered.

3.1. CONCENTRATION POLARIZATION

Consider first Equation. 5. Only independent variable is ξ and integrating once

$$U\phi = D\frac{d\phi}{d\xi} + C \tag{6}$$

where the constant of integration is found to be zero using the boundary conditions that as $\xi \rightarrow \infty$ (interior of the oil phase), ϕ and $d\phi/d\xi \rightarrow 0$. One has

$$U\phi = D\frac{d\phi}{d\xi} \tag{7}$$

Now, instead of solving the equation for conservation of solvent in the oil phase Butler and Mokrys (1989) assume effectively a solution in the form

$$U\phi = -D\frac{d\phi}{d\xi} \tag{8}$$

Adding Equations. 7 and 8 we get $2U\phi = 0$ or $\phi = 0$, a result that cannot be used. Ignoring Equation. 8 and integrating Equation. 7 we get

$$\phi = \phi_o e^{\int \frac{U}{D} d\xi} \tag{9}$$

However, a look at Figures 2.1 and 3.1 shows that U is expected to be positive, that is, the interface recedes. Hence, Equation. 9 appears unreasonable as it shows that the solvent concentration increases into the oil phase, and this form of approximation is discarded.

3.2 BOUNDARY LAYER THEORY

If in Equation. 4 V_p is replaced with η component of V_z then one has $V_p = \sin\theta . V_z$ where V_z is given in Equation. 2 and the inclination θ between η and z is shown in Figure. 3.1, then

$$\frac{\partial}{\partial \eta}[\frac{k\Delta\rho g.\sin\theta}{\mu}\phi] = \frac{\partial}{\partial \xi}[D\frac{\partial \phi}{\partial \xi}] \tag{10}$$

is obtained. At this point, the slender body approximation (Batchelor, 1967) is invoked where the shape of the interface, sin θ here, changes only slowly with η. Assuming further that μ is a constant in the ribbon and infinite outside, and D is constant inside the ribbon and zero outside, one has

$$\frac{k\Delta\rho g\sin\theta}{\mu D}\frac{\partial}{\partial\eta}\phi=\frac{\partial^2\phi}{\partial\xi^2} \tag{11}$$

in the ribbon. Equation. 11 has a solution (Bird et al, 2002)

$$\phi=\phi_o erfc\frac{\xi}{\sqrt{4\mu D\eta/k\Delta\rho g\sin\theta}} \tag{12}$$

where *erfc* is the complimentary error function. It is now possible to determine several quantities following Butler and Mokrys (1989). The thickness of the ribbon δ is given by

$$\phi_{\min}=\phi_o erfc\frac{\delta}{\sqrt{4\mu D\eta/k\Delta\rho g.\sin\theta}}=\phi_o erfc(u) \tag{13}$$

where $\phi_{\min}$ is the solvent volume fraction on the inner edge of the ribbon taken to be $\phi_{\min}/\phi_o$ 0.01. The assumption is similar to that used by Butler and Mokrys (1989) though not identical. The variable u is defined in Equation. 13 leads to u = 1.8225 and $\delta\sim 1.8225\sqrt{4\mu D\eta/k\Delta\rho g\sin\theta}$. The flow rate of oil collected at the bottom is

$$Q_b'=\int_0^{\delta}V_p(1-\phi)d\xi\Big|_{z=h} \tag{14}$$

Substituting for ϕ from Equation. 1 and integrating after changing the variable from ξ to the argument on the right hand side of Equation. 12 and integrating, one has

$$Q_b'=2.\sin\theta\sqrt{\frac{k\Delta\rho gDh}{\mu}}[(1-\phi_o)u+\phi_o(u.erf(u)+\frac{(e^{-u^2}-1)}{\sqrt{\pi}})] \tag{15}$$

where Q_b' is the flow rate in the ribbon tangential to the interface. An assumption has been made that $\eta=N=\sin\theta.h$ at the bottom. To get the normal component (z-component),

which is the flow rate out of the box in Figure 3.1, the right hand side is divided by sin θ to get

$$Q_b = 2\sqrt{\frac{k\Delta\rho gDh}{\mu}}[(1-\phi_o)u + \phi_o(u.erf(u) + \frac{(e^{-u^2}-1)}{\sqrt{\pi}})] \qquad (16)$$

where h is the total height of the system shown in Figure 3.1. The quantity within square brackets is only a number. The above steps shows that the value of sin θ used in the calculations is an average value. It can also be shown that all approximations become exact if sin θ is a constant in which case the interface in Figure 3.1 is given by a straight line. Now, Butler and Mokrys (1989) verified their results experimentally by comparing Q_b with $\sqrt{h}$ and a straight line was obtained. Equation. 16 also shows the same. The solvent lost is

$$q_b = 2\phi_o\sqrt{\frac{k\Delta\rho gDh}{\mu}}[u - (u.erf(u) + \frac{(e^{-u^2}-1)}{\sqrt{\pi}})] \qquad (17)$$

which decreases as the solubility decreases. To derive Equation. 17 the term (1- ϕ) in Equation. 14 was replaced with ϕ. The exit volume fraction ϕ_e is given by $q_b/(Q_b+q_b)$ or

$$\phi_e = \phi_o[u - (u.erf(u) + \frac{(e^{-u^2}-1)}{\sqrt{\pi}})]/u \qquad (18)$$

Since u = 1.8225, it leads to ϕ_e = 0.3084 which is oil much leaner in solvent than the saturation concentration.

4. CONCENTRATION DEPENDENT TRANSPORT

The transport and thermodynamic properties are very sensitive to solvent concentrations and this feature need to be introduced to see what it does to the previous result that the oil at the production well is supersaturated with solvent. Previously we have argued and found that the simplest concentration dependence of the diffusivity can be put down as

$$D = D_o e^{\alpha\phi} \tag{19}$$

The constant α is large and of the order of 10. Since the viscosity has about inverse relation to diffusivity, it is modeled as

$$\mu = \mu_o e^{-\alpha\phi} \tag{20}$$

Tran et al (2012) used free volume theory to express the transport properties of CO_2 in heavy crude. In general, the diffusivity D and viscosity μ there has inverse relationship. The diffusivity values were predicted after determining parameters from the viscosity values as function of CO_2 concentrations. The predicted diffusivities were found effectively to follow Equation. 19, and hence, Equation. 20 follows. This inverse relation is easily seen in Stokes-Einstein equation as well.

If volumes are additive $\Delta\rho = (1-\phi).\rho_o + \phi\rho_{sL} - \rho_{sV}$ where ρ_o is the density of pure oil, ρ_{sL} is the density of pure solvent dissolved in oil ("condensed phase") and ρ_{sV} is the density of pure solvent in vapor form (as introduced). It can be rewritten as

$\Delta\rho = (\rho_o - \rho_{sV}) + \phi.(\rho_o - \rho_{sL})$. Of these ρ_o and ρ_{sL} are similar (see Mohan et al, 2017a) and the last term can be ignored. Further, as $\rho_o >> \rho_{sV}$, $\Delta\rho \simeq \rho_o$.

4.1. FORMULATION

On using these, Equation. 10 becomes

$$\frac{\partial}{\partial\eta}[\frac{k\rho_o g e^{\alpha\phi}.\sin\theta}{\mu_o}\phi] = \frac{\partial}{\partial\xi}[D_o e^{\alpha\phi}\frac{\partial\phi}{\partial\xi}] \tag{21a}$$

The term sin θ can be taken to be a constant in the neighborhood. Using this information Equation. 21a becomes

$$\frac{k\rho_o g\sin\theta}{D_o\mu_o}\frac{\partial}{\partial\eta}[e^{\alpha\phi}\phi] = \frac{\partial}{\partial\xi}[e^{\alpha\phi}\frac{\partial\phi}{\partial\xi}] \tag{21b}$$

which differs from Equation. 11 by the exponential terms. We can now look the following transform, $s = \frac{\xi}{\sqrt{4\mu_o D_o\eta / k\rho_o g\sin\theta}}$, which using chain rule leads to

$$-2s\frac{d}{ds}[e^{\alpha\phi}\phi] = \frac{d}{ds}[e^{\alpha\phi}\frac{d\phi}{ds}] \tag{21c}$$

It is possible to differentiate both sides of Equation. 21c to get

$$\frac{d^2\phi}{ds^2} = -\alpha[(\frac{d\phi}{ds})^2 + 2s\phi\frac{d\phi}{ds}] - 2s\frac{d\phi}{ds} \tag{22}$$

Equation. 22 is subject to the boundary conditions that $\phi = \phi_o$ at $s = 0$ and $\phi \to 0$ as $s \to 0$. The numerical solutions were obtained using finite differences (central difference) Figure. 4.1 for $\alpha\phi_o$ = 0 (concentration independent diffusivity), $\alpha\phi_o = \infty$ and $\alpha\phi_o$ = 10. The first two cases have analytical solutions of

$$\phi = \phi_o erfc(s) \; for \; \alpha\phi_o = 0 \tag{23a}$$

$$\phi = \phi_o \exp(-s^2) \; for \; \alpha\phi_o = \infty \tag{23b}$$

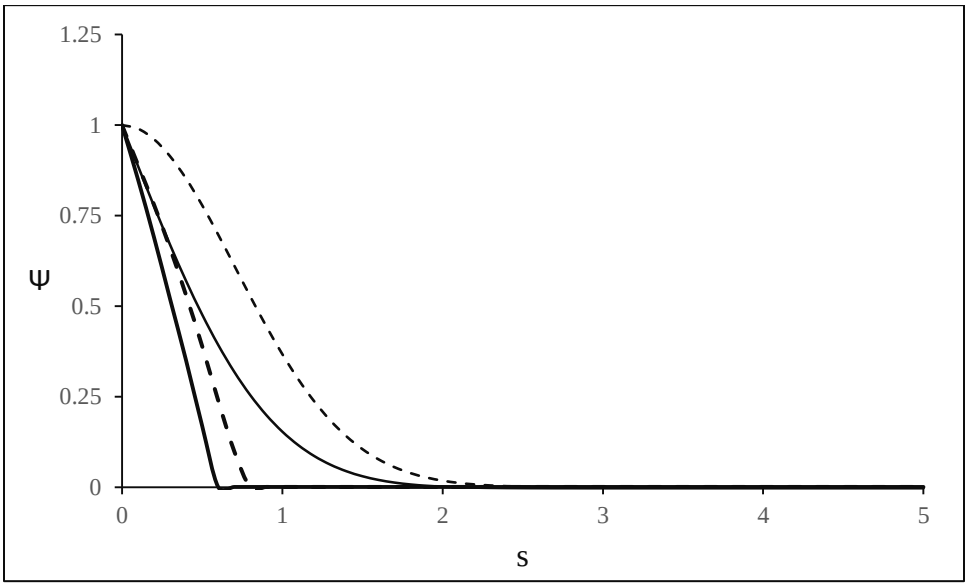

Figure 4.1. Numerical solution for Equation. 22 using central finite difference for $\alpha\phi_o$ = 0 (thin line), $\alpha\phi_o = \infty$ (thin dashed line), $\alpha\phi_o$ = 3(thick dashed line) and $\alpha\phi_o$ = 10(thick line).

It is now possible to obtain a boundary layer from

$$\delta = \int_{\phi_o}^{0} \xi d\phi \Big/ \int_{\phi_o}^{0} d\phi \tag{24}$$

or in dimensionless quantities

$$u = \int_{0}^{1} s d\psi \tag{25}$$

which was obtained numerically. Here, $\psi = \phi / \phi_o$. It leads to 0.886 for $\alpha\phi_o = \infty$, 0.3075 for $\alpha\phi_o = 10$, 0.40825 for $\alpha\phi_o = 3$ and 0.565 for $\alpha\phi_o = 0$. That is, not much range in the values of *u*.

4.2. IMPACT ON EXIT CONCENTRATIONS

Following developments of Equations. 14-17, we have

$$Q_b = 2\sqrt{\frac{k\Delta\rho gDh}{\mu}}\int_0^u e^{\alpha\phi_o\psi}(1-\phi_o\psi)d\psi \tag{26}$$

and

$$q_b = 2\phi_o\sqrt{\frac{k\Delta\rho gDh}{\mu}}\int_0^u e^{\alpha\phi_o\psi}.\psi ds \tag{27}$$

The integrals in Equations. 26 and 27 can be called I_1 and I_2. Finally, the exit concentrations are calculated. These are shown in Table 4.1.

Table 4.1. Exit concentration calculated using numerical solution of Equations. 26 and 27.

	$\alpha\phi_o = 0$	$\alpha\phi_o = 3$	$\alpha\phi_o = 10$	$\alpha\phi_o = \infty$
U	0.565	0.408	0.307	NA
I_1	$0.565 - 0.394\phi_o$	$9.6264 - 4.0298\phi_o$	$1718.508 - 1598.228\phi_o$	NA
I_2	$0.394\phi_o$	$4.0298\phi_o$	$1598.228\phi_o$	NA
ϕ_e / ϕ_o	0.69	0.41	0.93	NA

5. MODELING THE REMAINDER

The remaining issues deal with locating the oil-gas interface, dealing with reservoir heterogeneity and with asphaltene precipitation. Again, these issues are dealt with in a simplified fashion, as a consequence only outlines are provided. The important issues of partial displacement in this case where the flow is mainly tangential and not only normal to the interface, are neither clarified nor included.

5.1. SHAPES OF THE INTERFACE

Consider a point given as P* which is the origin of the $\eta - \xi$ coordinate shown in Figure 5.1. The whole figure is mapped by $x - z$ system and P* is given by x^*, z^*.

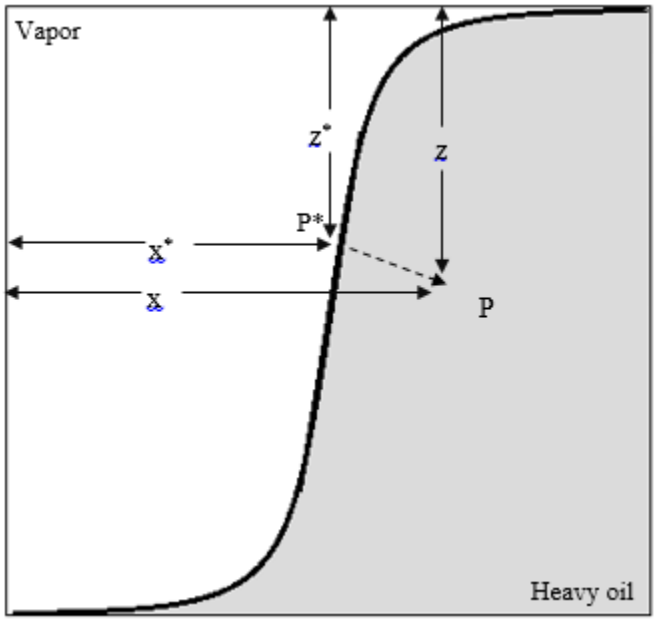

Figure 5.1. The relation between the two coordinates, $x - z$ and η - ξ are shown. The dashed line is the ξ direction.

The two jump balances due to mass transfer at the interface are

$$\dot{m} = c(V_\xi - \sigma) - D_o e^{\alpha\phi} \frac{\partial c}{\partial \xi} \text{ at the interface} \tag{28}$$

where $\dot{m}$ is the rate of mass of the solvent transferred from the gas phase into the liquid phase and *c* is the solvent concentration in the liquid. The total mass transferred is

$$\dot{m} = \rho(V_\xi - \sigma) \text{ at the interface} \tag{29}$$

where ρ is the total density which from before is $\rho = (1-\phi).\rho_o + \phi\rho_{sL}$. It is being assumed here that only solvent can move from one phase to another but the oil cannot. Eliminating $\dot{m}$ between the two, and replacing variables by their values at the interface, and multiplying the whole equation with $v_L = 1/\rho_{sL}$ the constant mass density of the solvent in the liquid phase, one has

$$\sigma = U - \frac{D_o e^{\alpha\phi}}{v_L \rho_o (1-\phi)} \frac{\partial \phi}{\partial \xi} \tag{31}$$

where σ is the interfacial velocity normal to the interface. Note that $dz^*/dx = \tan\theta$. It leads to

$$\sigma = V_z^* \cos\theta + D_o e^{\alpha\phi_o} \sqrt{\frac{\pi\mu_o D_o z^*}{k\rho_o g}} \tag{32}$$

where the star superscript has been added to V_z to indicate that the physical properties used to calculate this quantity are all evaluated at the interface at solvent concentration ϕ^*. In Figure 4.1, we find that the slope of the concentration profile at the origin is same for the cases of $\alpha\phi_o$ = 10 and $\alpha\phi_o$ = 0. For the latter case, the slope at *s* = 0 can be found

analytically from Equation. 23a as $\sqrt{\pi\mu_o D_o z^* / k\rho_o g}$. This is substituted on the right hand side in Equation. 32 to get Equation. 31. Now, this the kinematic boundary conditions that lead to (Higgins et al, 1977)

$$\sigma = \frac{\partial z^* / \partial t}{\sqrt{1 + (\partial z^* / \partial x)^2}} \tag{33}$$

where the equation of the interface is given by $z = z^*(x,t)$.

The following algorithm can be used: if the shape *z** is known at time *t*, then the slopes $\partial z^* / \partial x$ can also be determined. Then using Equation. 33, the shape of the interface at a later time can also be found using finite difference/forward difference in time: $\frac{\partial z^*}{\partial t} = \frac{z^*(x, t+\Delta t) - z^*(x,t)}{\Delta t}$. That is, *z** at fixed *x*, is updated.

5.2. RESERVOIR HETEROGENEITY

This is a problem that was addressed by Shi and Leung (2014). Let the permeability be

$$k(x,z) = k_o . w(x,z) \tag{34}$$

Equation. 21b becomes

$$\frac{k_o \rho_o g}{D_o \mu_o} \frac{\partial}{\partial \eta} [\sin\theta . w . e^{\alpha\phi} \phi] = \frac{\partial}{\partial \xi} [e^{\alpha\phi} \frac{\partial \phi}{\partial \xi}] \tag{35}$$

It is straightforward to obtain a numerical solution to Equation. 35, but it is necessary to relate (η, ξ) to (x, z) if only because permeability is available as a function $w(x, z)$ whereas $w(\eta, \xi)$ is not needed.

We begin by saying that the equation of the interface $z = z^*(x)$ is known. To locate the point P* in Figure 5.1 we start by line integration from the top right corner to get $\eta^* = \int_{x^*}^{L} \sqrt{1+(\partial z^*/\partial x)^2}.dx$ where L is the total length in x-direction. Hence, the coordinates of P*, a point on the interface is known as $(\eta^*, 0)$. From here, we would like to find (η, ξ) for the point P in the interior. The point P is on the line perpendicular to the interface at P* as shown in Figure 5.1. In this case, the ξ value there is

$$(x-x^*)^2 + (z-z^*)^2 = \xi^2 \tag{36}$$

where (x, z) in Equation. 36 provides the location of P which is also given by (η^*, ξ). Note that both P and P* share the same value of η.

It remains to show how the perpendicular at the interface is drawn. From Higgins et al (1977) this unit normal is given by

$$\boldsymbol{n} = \frac{\boldsymbol{e}_z - \dfrac{\partial z^*}{\partial x}\boldsymbol{e}_x}{\sqrt{1+(\dfrac{\partial z^*}{\partial x})^2}} \tag{37}$$

where $\boldsymbol{e}_x$ and $\boldsymbol{e}_z$ are two unit vectors in the two directions and $dz^*/dx = \tan\theta$. The remaining procedure for getting Q_b, q_b and x_e remain unchanged. However, the mapping needs to be upgrades whenever the shape of the interface changes.

5.3 ASPHALTENE PRECIPITATION

A key problem is that the kinetics of asphaltene precipitation is not known. If it can be assumed that the asphaltene precipitation is faster than the rate of displacement, then a model can be made where the asphaltene precipitates instantaneously when the solvent

concentration $\phi = \phi_c$ is reached. The result is straightforward. The outer edge of the ribbon at $\phi = \phi_o$ now becomes $\phi = \phi_c$. It can also be assumed that the volume fraction of oil on precipitating asphaltene is $1 - f$ and the volume fraction of asphaltene is f and below 0.15. Now in the gas phase at the top, the viscosity of the gas is very low and hence even on reduction of porosity for ε to $\varepsilon(1-f)$ there will not be much pressure drop. After precipitation of asphaltene the oil that is left behind is a light oil with a different solubility $\phi^* > \phi_c$. However, this band which is light oil with low viscosity, will drain faster and disappear, leaving only two phases, gas and oil with an interface at ϕ_c. There is a special case where the new void volume fraction $\varepsilon(1-f)$ approaches low values that the flow in gas phase is choked.

6. RESULTS AND DISCUSSION

We have analyzed the basic conservation equations for the solvent in oil and their solutions to determine the gravity drainage of the solvated heavy oil. Butler and Mokrys (1989) start with a reasonable but assumed concentration profile, but our analysis shows that this form to be unsuitable. The one that is suitable, gives us governing equation that is similar to the boundary layer equation, but provides a result for the oil recovered that is very similar to the final result of Bulter and Mokrys (1989). The condition $\frac{V_p}{N} >> \frac{U}{\delta}$ for the present solution, can now be determined as $\frac{\delta}{N} >> \frac{\cos\theta}{\sin\theta}$ on using $V_p = \sin\theta . V_z$ and $U = \cos\theta . V_z$. Further simplification can be made with $h \simeq N / \sin\theta$ to get $\frac{\delta}{h} >> \frac{\cos\theta}{\sin^2\theta}$. At small times θ starts from $\sim 90^o$, that is the inequality is satisfied (see for instance the dynamics of Hele-Shaw cell in Bulter and Mokrys (1989). At large times the boundary layer thickness increases and it could also be satisfied. h is a constant. Thus, the basic assumption remains valid.

We have taken into account that the diffusivity and viscosity of solvated heavy oil are strongly dependent on solvent concentrations. The concentration profiles for $\alpha\phi_o = 10$ differs from that of $\alpha\phi_o = 0$ (the case of no concentration dependence) in Figure 4.1, by the fact the solvent penetrates into oil much less when the concentration dependence is introduced (Tran et al, 2012). Note that we have removed somewhat arbitrary assumption that $\phi_{\min} = 0.01$ defines the end of the boundary layer. Further, the solvent concentration profile falls very sharply to zero (Mohan et al, 2017b). The case of $\alpha\phi_o = \infty$ is of interest

only because it remains bounded, however, as we lose both the main convection and diffusion terms in that limit, it has little physical meaning. The main result of including concentration dependence in diffusivity is to the reduction in solvent penetration (lower value of *u*). The flow rate of oil increases enormously, see Table 4.1. This happens because the viscosity is greatly reduced, due to the exponential term in Equation. 26. Hence the basic idea of using a solvent to improve oil recovery by lowering the viscosity does appear to work, but has some caveats as explained below.

Besides the above we have also calculated the concentration of solvent in the exit stream. We find it to be large in Table 4.1 for concentration dependent transport properties. This happens because the solvent concentration profile for $\alpha\phi_o$ = 10 in Figure.4.1 is of a type where the oil can be sliced into two parts: a nearly saturated slice (of thickness *u*) and the rest is dry. Now, only the nearly saturated slice will move under gravity and the dry region will not move because of its high viscosity. Consequently, it is not surprising that the exit oil is nearly saturated. Thus, if the solvent is fully soluble, that is, $\phi_o = 1$ then the oil that is recovered is mostly the solvent. See the exit concentration in Table 4.1. These is a scope for optimizing the solubility of the solvent. As noted earlier, Mohan et al (2017b) found $\alpha\phi_o$ ~ 10 for hexane, heptane and toluene in heavy oil, for which ϕ_o = 1, thus $\alpha\phi_o$ ~10 in their case. Tran et al (2012) saw α ~ 35 for CO_2 in oil, but the highest value of ϕ_o ~ 0.35 for gas pressure of 3000 psi. So the highest value of $\alpha\phi_o$ ~ 10, but can often be much lower. As a result, in Table 4.1 we have also presented calculations of $\alpha\phi_o$ = 3: the drainage/recovery is lower but the loss of solvent is much lower.

We have also outlined how a few other problems can be solved using this framework. For instance the method for updating the position has been shown. We tried a simple case $dz^*/dx = \tan\beta$ where β is a constant, that is, equation of a straight line, as the initial profile and updated it by integrating Equations. 33 and 34. We a get a profile that is too complicated to interpret and this result has not been included. The reservoir heterogeneity is quite different issue being lengthy and complex. We suggest that for such a system, this approach be abandoned for a numerical method for a moving boundary problem involving mass transfer in $x-z$ coordinates. Packages exist now which make such calculations feasible with less restrictions (Tran et al, 2015). Finally, there is the issue of asphaltene precipitation. There is lot about it that is not known. A solution has been provided that simplifies the system by a large amount, but yet preserves some real features.

7. CONCLUSIONS

We see here that the basic idea of using a solvent to lower the oil viscosity such that there is a good amount of recovery, does indeed hold. However, if the solvent has a good solubility in oil then the oil recovered will be mostly solvent. There is a good possibility of optimizing the choice of solvent, although there is no known relation between solubility and its ability to reduce viscosity of oil. We have also analyzed the conservation of species equation following conventional procedures which disagrees with the Butler-Mokrys formulation but agree with their final results, that flow rate of oil recovered varies with $\sqrt{h}$ where h is the depth of the reservoir. However, looking at the fundamentals we are also able to show how, the shape of interface would change with time, on how the reservoir heterogeneity can be included and provided a first approximation solution for the case where asphaltene precipitation takes place.

REFERENCES

Batchelor, G.K. (1967) An Introduction to Fluid Dynamics, Cambridge University Press, Cambridge, p.463.

Banerjee, D.K. (2012) Oil Sands, Heavy Oil & Bitumen, Penn Well, Tulsa, p.57.

Bachu, S., and Shaw, J. (2003) Evaluation of CO_2 sequestration capacity in Alberta's oil and gas reservoirs at depletion and the effect of underlying aquifers. Journal of Canadian Petroleum Technology, 42, 51-61.

Bird, R.B., Stewart, W.E., and Lightfoot, E.N. (2002) Transport Phenomena, John Wiley, New York, p. 559-560.

Burke, N.E., Hobbs, R.E., and Kshou, S.F. (1990) Measurement and modeling of asphaltene precipitation. Journal of Petroleum Technology, 42, 1440-1520.

Butler, R.M., and Mokrys, I.J. (1989) Solvent analog model of steam-assisted gravity drainage, AOSTRA Journal of Research. 5, 17-32.

Butler, R.M., and Mokrys, I.J. (1991) A new process (VAPEX) for recovering heavy oils using hot water and hydrocarbon vapor, The Journal of Canadian Petroleum Technology, 30,1, 97-106.

Chung, F.T.H., Jones, R.A., and Nguyen, H.T. (1988) Measurements and correlations of the physical properties of CO_2/heavy-crude-oil mixtures. SPE Reservoir Engineering, 3, 822-8.

Haghighat, P., and Maini, B.B. (2010) Role of asphaltene precipitation in VAPEX process Journal of Canadian Petroleum Technology, 49, 14-21.

Higgins, B.G., Silliman, W.J., Brown, K.A., and Sriven, L.E. (1977) Theory of meniscus shape in film flows. A synthesis. Industrial and Engineering Chemistry Fundamentals, 16, 393-401.

Mohan, V., Neogi, P., and Bai, B. (2017a) Flory-Huggins solution for heavy oils. The Canadian Journal of Chemical Engineering, 95, 796-798.

Mohan, V., Neogi, P., and Bai, B. (2017b) Concentration dependent diffusivities of model solvents in heavy oil. Under journal review.

Nghiem, L.X., and Coombe, D.A. (1997) Modeling asphaltene precipitation during primary depletion. Society of Petroleum Engineering Journal, 2, 170-176.

Shaw, J., and Bachu, S. (2002) Screening, evaluation, and ranking of oil reservoirs suitable for CO_2-flood EOR and carbon dioxide sequestration, The Journal of Canadian Petroleum Technology, 41, 51-61.

Schlichting, H.(1968) Boundary-Layer Theory, 6th edition, McGraw-Hill, New York, p. 118, 264.

Shi, J., and Leung, J.Y. (2014) Semi-analytical proxy for Vapex process modeling in heterogeneous reservoirs. Journal of Energy Resources Technology, 136, 032904-1-13.

Tran, T.Q.M.D., Neogi, P., and Bai, B. (2012) Free volume estimates of thermodynamic and transport properties. Chemical Engineering Science 80, 100-108.

Tran, T.Q.M.D., Neogi, P., and Bai, B. (2015) A single pore model for displacement of heavy crude oil with carbon dioxide. Society of Petroleum Engineers. 21, 864-872.

SECTION

2. CONCLUSIONS AND FUTURE WORKS

2.1 CONCLUSIONS

This discourse offers in depth the significance of mass transfer, thermodynamics and fluid flow effect on solvent and heavy oil interaction during recovery of heavy oil. Liquid and gaseous solvents minimizes viscosity of heavy oil expediting recovery process along with swelling of oil and with or without asphaltene precipitation.

Solvents as it solubilizes in heavy oil causes swelling of oil and asphaltene precipitation. First paper involved modeling the swelling characteristic and asphaltene precipitation of heavy oil in the presence of gaseous solvents with pressure using Flory-Huggins theory. The results of the model is fitted well with experimental data.

Diffusivity plays a major role when solvents solubilize in heavy oil. Diffusivity can be concertation dependent. Second paper deals with measuring the concentration dependence of diffusivity while using liquid solvents to bring down the viscosity heavy oil. Dissolution and desorption experiments are conducted. The results proved that diffusivity is highly concentration dependent.

Using solubility and diffusivity concentration dependence, a model is created to predict optimum solvent in third paper. In a process like VAPEX process, concentration dependence of solvents are found to have an effect on solvent penetration in heavy oil and drainage of heavy oil. Conservation equation in heavy oil extraction process is remodeled to an appropriate one. Higher the concentration dependence, drained oil is saturated with solvent, less concentration dependence drained oil had less exit solvent concentration.

2.2 FUTURE WORKS

The above studies can be further extended by the following proposition

- Diffusion coefficient at infinite dilution needs to be measured.
- Residual oil when the flow is tangential to the interface (as in VAPEX) needs to be determined
- Kinetics of asphaltene precipitation needs to be studied.

REFERENCES

Aguiar, J.I.S and Mansur, C.R.E. (2015) Study of the interaction between asphaltenes and resins by micocalorimetry and ultraviolet –visible spectroscopy, Fuel, 140, 462-469.

Alagorni, A.H. Yaacob,Z.B. and Nour, A.H. (2015) An overview of oil production stages: Enhanced oil recovery techniques and nitrogen injection, International Journal of Environmental Science and Development, 6, 9, 693-701.

Banerjee,D.K. (2012) Oil Sands, Heavy Oil and Bitumen, From Recovery to Refinery, Penn Well Corp, Tulsa.

Butler, R.M. (1991) Thermal Recovery of Oil and Bitumen, Prentice Hall, New Jersey, p. 285-359.

Craig, F.F. (1971) The Reservoir Engineering Aspects of Water flooding, American Institute of Mining, Metallurgical and Petroleum Engineers Inc, Dallas.

Gray, M.R. (2015) Upgrading Oil sands Bitumen and Heavy Oil, The University of Alberta Press, Alberta, p. 296-309.

Hein, F.J. (2006) Heavy Oil and Oil (Tar) Sands in North America: An Overview & Summary of Contributions, Natural Resources Research, 15, 2, 67- 84.

Nehring, R., Hess, R., and Kamionski, M. (1983) The Heavy Oil Resources of the United States, Santa Monica, Rand Corporation, p. 35.

Larry, L.W. (1989) Enhanced Oil Recovery, Prentice Hall, New Jersey.

Papavinasam, S. (2014) Corrosion Control in the Oil and Gas Industry, Elsevier, Oxford, p.62-65.

Speight, J.G. (2004) Petroleum Asphaltenes Part1-Asphaltnes, Resins and the structure of petroleum, Oil & Gas Science and Technology – Rev. IFP, 59, 5, 467-477.

Speight, J.G. (2009) Enhanced Recovery Methods for Heavy Oil and Tar Sands, Gulf Publishing House, Houston , p. 77,82.

Subramanian, M., Deo, M.D., and Hanson, F.V. (1996) Compositional Analysis of Bitumen and Bitumen-Derived Products, Journal of Chromatographic science, 34, 20-26.

Thomas, S. (2008) Enhanced oil recovery- An overview, Oil & Gas Science and Technology – Rev.IFP, 63, 19-19.

Green.D.Q., and Willhite, G,P. (1998) Enhanced oil recovery, SPE Textbook Series, Vol.6, Richardson, p. 1,2.

VITA

Vijitha Mohan holds a B.Tech degree from University of Madras, India, an M.S degree from Mississippi State University and a PhD from Missouri University of Science and Technology obtained in May 2017, all in Chemical Engineering. M.S research was based on ester bond lopping from phospholipids and surface modification of polymers. Ph.D. research included mass transfer studies during heavy oil recovery process.